Table 1 Clinical features of patients

Variables			No. or mean ± SD	(%)	Range
Age	(years)		64.2 ± 11.9		
Sex	(male/female)		149/92	(61.8/38.2)	
Background		HBV	48	(19.9)	
		HCV	152	(63.1)	
		HBV + HCV	3	(1.2)	
		Alcoholism	21	(8.7)	
		NAFLD	5	(2.1)	
		PBC	6	(2.4)	
		AIH	1	(0.4)	
		Unknown	5	(2.2)	
		CH/LC	187/54	(77.6/22.4)	
Treatment		UDCA	100	(41.5)	
		SNMC	6	(2.5)	
		BCAA	21	(8.7)	
Prior HCC treatment		Yes	92	(38.2)	
		No	149	(61.8)	
Prevalent HCC		Yes	36	(14.9)	
		No	205	(85.1)	
Alb	(g/dL)		4.1 ± 0.7		(2.1–5.3)
T-Bil	(mg/dL)		0.9 ± 0.5		(0.1–3.6)
ALT	(IU/L)		37 ± 30		(7–251)
GGTP	(IU/L)		58 ± 92		(10–944)
ALP	(IU/L)		316 ± 213		(120–2152)
ChE	(IU/L)		261 ± 115		(52–662)
PLT	(10^4/μL)		15.0 ± 5.9		(3.0–36.9)
PT	(%)		97 ± 18		(41–126)
NH3	(mg/dL)		67 ± 38		(14–210)
AFP	(ng/mL)		4.0 ± 2.3		(3.0–10.0)
DCP	(mAU/mL)		248 ± 1201		(6–13 497)
AFP-L3		Detectable	60	(24.9)	
		Average of detectable cases (%)*	10.9 ± 8.0		(3.9–48.0)

Average of detectable cases (%)*: average of percentage of fucosylated fraction of α-fetoprotein (AFP-L3%)value cases that could be detected ($n = 60$).

Alb, albumin; AFP, α-fetoprotein; AIH, autoimmune hepatitis; ALP, alkaline phosphatise; ALT, alanine aminotransferase; BCAA, branched chain amino acid; CH, chronic hepatitis; ChE, choline esterase; DCP, des-gamma-carboxy prothrombin; GGTP, gamma-glutamyltransferase; HBV, hepatitis B virus infection; HCV, hepatitis C virus infection; LC, liver cirrhosis (in this study, we defined LC as platelet count below 10^5/μL, unless previously proven with a histological method or clinically diagnosed); NAFLD, non-alcoholic fatty liver disease; NH3, ammonia; PBC, primary biliary cirrhosis; PLT, platelet count; PT, prothrombin time; SNMC, strong neo-minophagen C; T-Bil, total bilirubin; UDCA, ursodeoxycholic acid.

were found to be significant factors for detection of HCC in the future. From those results, we carried out multivariate analysis, and AFP-L3% lower than 5.75 ($P = 0.036$, hazard ratio 0.289) and female sex ($P = 0.024$, hazard ratio 0.171) were shown to be significant independent factors for earlier detection of HCC (Table 3).

Discussion

Treatment strategies for patients with HCC and their prognosis strongly depend on the tumor stage when first discovered. For successful radical treatment, detection of the tumor in the early stage is vital and various diagnostic imaging methods have been developed, whereas various tumor markers have also been investigated.

Guidelines for treatment of HCC in Japan have been presented by The Japan Society of Hepatology, who recommended the measurement of two HCC tumor markers in patients at high risk for HCC. However, the 18th Survey and Follow-up Study of Primary Liver Cancer in Japan reported that most patients with HCC had an AFP level under 15 ng/mL and measurement of the AFP-L3 fraction in such cases was not possible. In the present study, the fucosylated fraction of α-fetoprotein was measurable in patients with chronic liver disease, even when their serum AFP values were lower than 10 ng/mL, with the present novel automated immunoassay for AFP-L3. Furthermore, we determined the optimal cut-off value for the AFP-L3 fraction after production of a ROC curve and showed its value for predicting future detection of HCC.

It has been reported that AFP-L3 is an effective marker for early diagnosis,[10] recurrence rate,[11–13] biological malignancy,[14–17] and prognosis[18–20] in HCC patients with chronic liver disease. The optimal cut-off value for AFP-L3 was reported to be 15% in a study that used the conventional assay,[21] whereas Richard *et al.* reported that 10.9% was the proper cut-off value for early detection.[22] Also, Hayashi *et al.*[12] and Sterling *et al.*[23] reported the utility

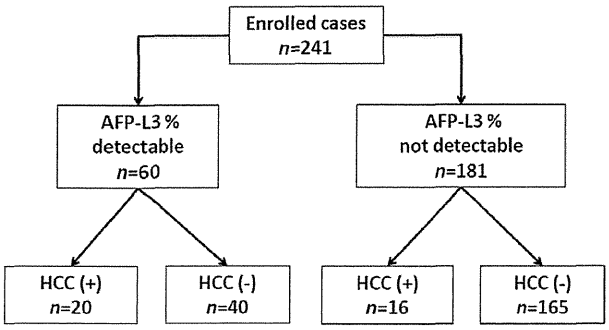

Figure 1 Grouping based on percentage of highly sensitive fucosylated fraction of α-fetoprotein (hs-AFP-L3%) and the presence of hepatocellular carcinoma (HCC). We measured α-fetoprotein (AFP), AFP-L3% and des-gamma-carboxy prothrombin in 241 patients. Each had a low AFP concentration (range 3–10 ng/mL) and 60 (24.9%) had detectable AFP-L3%, of whom 20 (33.3%) had HCC at the time of enrollment in the study. In addition, 16 (8.8%) of the 181 patients with undetected AFP-L3% had HCC.

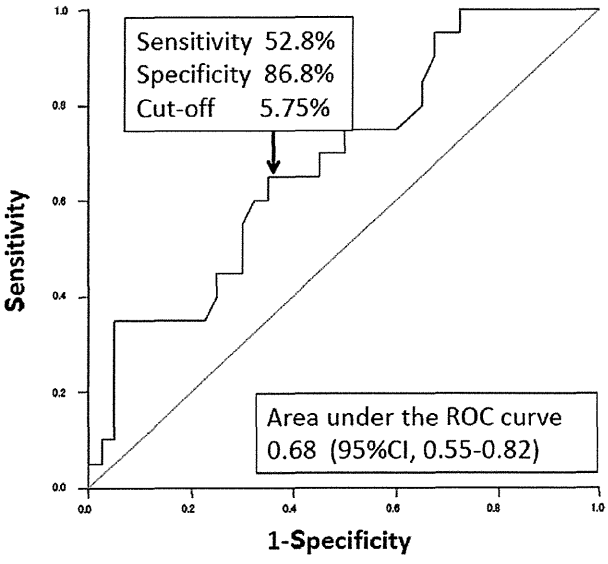

Figure 2 Receiver–operator characteristic (ROC) curve for percentage of highly sensitive fucosylated fraction of α-fetoprotein (hs-AFP-L3%) in patients with detectable AFP-L3%. The cut-off value for AFP-L3% is generally considered to range from 10–15%. For better accuracy as a tumor marker for hepatocellular carcinoma (HCC), we evaluated the optimal cut-off value of AFP-L3% in patients with low AFP using a ROC curve analyzing method. Our results showed an AFP-L3% cut-off value of 5.75% as a tumor marker for HCC, which had a sensitivity of 52.8% and specificity of 86.8%. With this condition, the area under the ROC curve was 0.68 (0.55–0.82, 95% CI).

of AFP-L3 measurement for prognosis and recurrence, with a cut-off value of 10%. Because the concentration of serum AFP was lower than 10 ng/mL in all cases enrolled in the present study, it might be inappropriate to compare our cut-off value with that of previous reports. Our findings suggest that the AFP-L3% cut-off

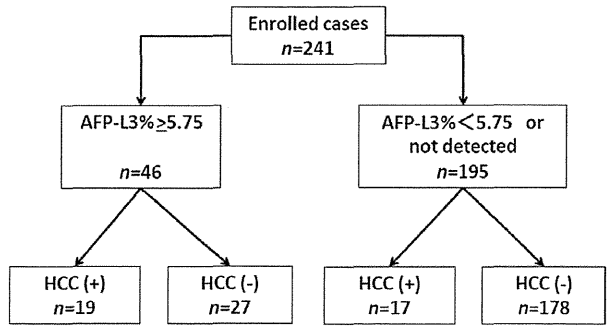

Figure 3 Grouping based on percentage of highly sensitive fucosylated fraction of α-fetoprotein (hs-AFP-L3%) with a cut-off value of 5.75% and presence of hepatocellular carcinoma (HCC). A total of 46 patients were AFP-L3% positive (over 5.75%), of whom 19 (41.3%) had HCC (true-positive group) and 27 did not (58.7%, false-positive group). In the AFP-L3% negative group, 17 (8.7%, false-negative group) of 195 had HCC.

Table 2 Comparison of scores as tumor marker for hepatocellular carcinoma

Tumor marker	Sensitivity (%)	Specificity (%)	PPV (%)	NPV (%)
AFP-L3% alone	52.8	86.8	41.3	91.3
DCP alone	58.3	89.5	56.8	90.1
AFP-L3% and/or DCP	77.7	85.6	48.3	93.9

AFP-L3%, percentage of fucosylated fraction of α-fetoprotein; DCP, des-gamma-carboxy prothrombin; NPV, negative predictive value; PPV, positive predictive value.

value should be 5.75% in cases with an AFP concentration below 10 ng/mL.

Several investigators have compared the sensitivity and specificity of various tumor markers for detection of HCC. In the present study, DCP was slightly superior as a tumor marker for HCC as compared with AFP-L3% measured by the μTAS-Wako i30. However, DCP and AFP-L3% might not be competitive markers, but rather compensative markers, because they reflect a different developmental form of HCC.[12]

Tamura *et al.* examined AFP-L3% using a μTAS-Wako i30 device in patients with HCC and benign liver disease.[24] They reported that AFP-L3% had the most accurate diagnostic power for HCC when the cut-off value was set at 7% in subjects with various serum levels of AFP. Since we enrolled only patients AFP below 10 ng/mL in our study, it may be reasonable that our cut-off value of 5.75% is superior.

Repeated imaging examinations such as computed tomography or ultrasonography are recommended at 3-month intervals for patients at high risk for HCC, because the mean doubling time of HCC is known to be about 3 months.[25] However, some investigators have expressed doubt regarding the value of such surveillance from the viewpoint of cost effectiveness. In our study, the detection rate of HCC during follow-up examinations in patients with a AFP-L3% value of 5.75% or more in serum was significantly

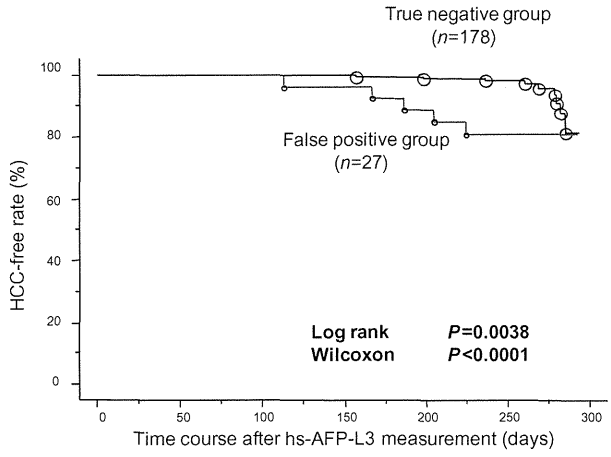

Figure 4 Comparison of hepatocellular carcinoma (HCC)-free rate between percentage of fucosylated fraction of α-fetoprotein (AFP-L3%) positive (≥ 5.75%) and negative (< 5.75% or not detected) groups after measurement of highly sensitive (hs)-AFP-L3% in patients who were not HCC free at the beginning of the present study. We followed the two groups presented in Figure 3, those with AFP-L3% of 5.75% or more (false-positive group, $n = 27$) and with AFP-L3% below 5.75% or not detected (true-negative group, $n = 178$) after their initial entry into the study. The median follow-up period was 230 days (186–270). During that period, HCC was newly detected in six patients in the false-positive group and 10 patients in the true-negative group. The HCC-positive rate was significantly higher in the false-positive group ($P = 0.00036$, χ^2-test, data not shown), whereas analysis with the Kaplan–Meier method showed that the HCC-free rate was also significantly higher in the false-positive group ($P = 0.0038$, log–rank test, $P < 0.0001$, Wilcoxon test, *respectively*).

Table 3 Multivariate analysis of factors affecting future occurrence of hepatocellular carcinoma (Cox's proportion-hazard model)

Factor	Hazard ratio	*P* value	95% Confidence interval
No liver cirrhosis	0.369	0.08	(0.12–1.12)
DCP < 40	0.764	0.679	(0.21–2.74)
AFP-L3% < 5.75	0.289	0.036	(0.09–0.93)
Female	0.171	0.024	(0.03–0.79)
Alb < 4.0	2.033	0.2487	(0.61–6.79)
ALT > 30	0.828	0.75	(0.26–2.66)

AFP-L3%, percentage of fucosylated fraction of α-fetoprotein; ALB, albumin; ALT, alanine aminotransferase; DCP, des-gamma-carboxy prothrombin.

higher than that of those with a value lower than 5.75% (Fig. 4). Our findings indicate that it is important to develop an improved surveillance protocol for high-risk patients based on this highly sensitive AFP-L3% data.

Our study is limited by the selection bias of patients whose serum AFP concentrations ranged from 3 to 10 ng/mL. However, the measurement of AFP-L3% with the current method is only recommended for cases with a serum AFP concentration above 3 ng/mL and the reliability of the data would be limited if cases with a lower concentration had been enrolled.

In conclusion, we examined the usefulness of AFP-L3% as a tumor marker for HCC in patients with chronic liver disease and low AFP concentration (3–10 ng/dL). Our results suggest that this novel AFP-L3 assay is useful to detect HCC in patients at high risk for tumor development.

References

1 Di Bisceglie AM, Rustgl VK, Hoofnagle JH *et al.* NIH conference. Hepatocellular carcinoma. *Ann. Intern. Med.* 1988; **10**: 390–401.
2 Zaman SN, Melia VM, Johnson RD *et al.* Risk factors in development of hepatocellular carcinoma in cirrhosis: prospective study of 613 patients. *Lancet.* 1985; **15**: 1357–60.
3 Miyaaki H, Nakashima O, Kurogi M *et al.* Lens culinaris agglutinin-reactive α-fetoprotein and protein induced by vitamin K absence are potential indicators of a poor prognosis: a histopathological study of surgically resected hepatocellular carcinoma. *J. Gastroenterol.* 2007; **42**: 962–8.
4 Durazo FA, Blatt LM, Corey WG *et al.* Des-γ-carboxy prothrombin, α-fetoprotein and AFP-L3 in patients with chronic hepatitis, cirrhosis and hepatocellular carcinoma. *J. Gastroenterol. Hepatol.* 2008; **23**: 1541–8.
5 Kobayashi M, Kuroiwa T, Suda T *et al.* Fucosylated fraction of alpha-fetoprotein, L3, as a useful prognostic factor in patiens with hepatocellular carcinoma with special reference to low concentrations of serum alpha-fetoprotein. *Hepatol. Res.* 2007; **37**: 914–22.
6 Sassa T, Kumada T, Nakano S *et al.* Clinical utility of simultaneous measurement of serum high-sensitivity des-gamma-carboxy prothrombin and Lens culinaris agglutinin A-reactive alpha-fetoprotein in patients with small hepatocellular carcinoma. *Eur. J. Gastroenterol. Hepatol.* 1999; **11**: 1387–92.
7 Yoshida S, Kurokohchi K, Arima K *et al.* Clinical significance of Lens culinaris agglutinin-reactive fraction of serum alpha-fetoprotein in patients with hepatocellular carcinoma. *Int. J. Oncol.* 2002; **20**: 305–9.
8 Kawabata T, Wada HG, Watanabe M *et al.* "Electrokinetic Analyte Transport Assay" for alpha-fetoprotein immunoassay integrates mixing, reaction and separation on-chip. *Electrophoresis.* 2008; **29**: 1399–406.
9 Kagebayashi C, Yamaguchi I, Akinaga A *et al.* Automated immunoassay system for AFP-L3% using on-chip electrokinetic reaction and separation by affinity electrophoresis. *Anal. Biochem.* 2009; **388**: 306–11.
10 Toyoda H, Kumada T, Kiriyama S *et al.* Prognostic significance of simultaneous of three tumor markers in patients with hepatocelluar carcinoma. *Clin. Gastroenterol. Hepatol.* 2006; **4**: 111–7.
11 Marrero JA, Feng Z, Wang Y *et al.* Alpha-fetoprotein, des-gamma-carboxyprothrombin, and lectin-bound alpha-fetoprotein in early hepatocellular carcinoma. *Gastroenterology.* 2009; **137**: 110–8.
12 Hayashi K, Kumada T, Nakano S *et al.* Usefulness of measurement of Lens culinaris agglutinin-reactive fraction of alpha-fetoprotein as a marker of prognosis and recurrence of small hepatocellular carcinoma. *Am. J. Gastroenterol.* 1999; **94**: 3028–33.
13 Tateishi R, Shiina S, Yoshida H *et al.* Prediction of recurrence of hepatocellular carcinoma after curative ablation using three tumor markers. *Hepatology.* 2006; **44**: 1518–27.
14 Khien VV, Mao HV, Chinh TT *et al.* Clinical evaluation of lentil lectin-reactive alpha-fetoprotein-L3 in histology-proven hepatoellular carcinoma. *Int. Biol. Merkers.* 2001; **16**: 105–11.
15 Hagiwara S, Kudo M, Kawasaki T *et al.* Prognostic factors for portal venous invasion in patients with hepatocellular carcinoma. *J. Gastroenterol.* 2006; **41**: 1214–9.

16 Tada T, Kumada T, Toyoda H *et al.* Relationship between Lens culinaris agglutinin-reactive alpha-fetoprotein and pathologic features of hepatocellular carcinoma. *Liver Int.* 2005; **25**: 848–53.
17 Oka H, Saito A, Ito K *et al.* Collaborative Hepato-Oncology Study Group of Japan. Multicenter prospective analysis of newly diagnosed hepatocellular carcinoma with respect to the percentage of Lens culinaris agglutinin-reactive alpha-fetoprotein. *J. Gastroenterol. Hepatol.* 2001; **16**: 1378–83.
18 Tamura Y, Igarashi M, Suda T *et al.* Fucosylated fraction of alpha-fetoprotein as a predictor of prognosis in patients with hepatocellular carcinoma after curative treatment. *Dig. Dis. Sci.* 2010; **55**: 2095–101.
19 Toyoda H, Kumada T, Kaneoka Y *et al.* Prognostic value of pretreatment levels of tumor markers for hepatocellular carcinoma on survival after curative treatment of patients with HCC. *J. Hepatol.* 2008; **49**: 223–32.
20 Yamashita F, Tanaka M, Satomura S *et al.* Prognostic significance of Lens culinaris agglutinin A-reactive alpha-fetoprotein in small hepatocellular carcinomas. *Gastroenterology.* 1996; **111**: 996–1001.
21 Tateishi R, Yoshida H, Matsunaga Y *et al.* Diagnostic accuracy of tumor markers for hepatocellular carcinoma: a systematic review. *Hepatol. Int.* 2008; **2**: 17–30.
22 Sterling RK, Jeffers L, Gordon F *et al.* Utility of lens culinaris agglutinin-reactive fraction of alpha-fetoprotein and des-gamma-carboxy prothronbin, alone or in combination, as biomarkers for hepatocellular carcinoma. *Clin. Gastroenterol. Hepatol.* 2009; **7**: 104–13.
23 Sterling RK, Jeffers L, Gordon F *et al.* Clinical utility of AFP-L3% measurement in North American patients with HCV-related cirrhosis. *Am. J. Gastroenterol.* 2007; **102**: 2196–205.
24 Tamura Y, Igarashi M, Kawai H *et al.* Clinical advantage of highly sensitive on-chip immunoassay for fucosylated fraction of alpha-fetoprotein in patients with hepatocellular carcinoma. *Dig. Dis. Sci.* 2010; **55**: 2576–83.
25 Woo HY, Jang JW, Choi JY *et al.* Tumor doubling time after initial response to transarterial chemoembolization in patients with hepatocellular carcinoma. *Scand. J. Gastroenterol.* 2010; **45**: 332–9.

HEPATOLOGY
Official Journal of the American Association for the Study of Liver Diseases

STEATOHEPATITIS/METABOLIC LIVER DISEASE

Real-Time Tissue Elastography for Evaluation of Hepatic Fibrosis and Portal Hypertension in Nonalcoholic Fatty Liver Diseases

Hironori Ochi,[1] Masashi Hirooka,[1] Yohei Koizumi,[1] Teruki Miyake,[1] Yoshio Tokumoto,[1] Yoshiko Soga,[2] Fujimasa Tada,[1] Masanori Abe,[1] Yoichi Hiasa,[1] and Morikazu Onji[1]

The aim of this study was to prospectively measure liver stiffness with real-time tissue elastography in patients with nonalcoholic fatty liver diseases (NAFLD) and to compare the result with the clinical assessment of fibrosis using histological stage. One hundred and eighty-one prospectively enrolled patients underwent real-time tissue elastography, with the first 106 being analyzed as the training set and the remaining 75 being evaluated as the validation set. Hepatic and splenic elastic ratios were calculated and compared with stage of histological fibrosis. Portal hypertension (PH) was assessed. Real-time tissue elastography cut-off values by stage in the training set were 2.47 for F1, 2.67 for F2, 3.02 for F3, and 3.36 for F4. Using these cut-off values, the diagnostic accuracy of hepatic fibrosis in the validation set was 82.6%-96.0% in all stages. Only portal fibrosis correlated with the hepatic elastic ratio by multivariate analysis. The area under the receiver operating characteristic curve of elastic ratio better correlated than serum fibrosis markers in both early and advanced fibrosis stages. Patients with PH, defined by splenic elasticity, had early fibrosis. Patients with severe PH were found only in the group with cirrhosis. *Conclusion:* Real-time tissue elastography is useful in evaluating hepatic fibrosis and PH in patients with NAFLD. (HEPATOLOGY 2012;1271-1278)

Nonalcoholic fatty liver disease (NAFLD) is currently one of the more common types of chronic liver disease (CLD) in many countries around the world.[1-3] It is thought that NAFLD is a component of metabolic syndrome and is associated with the deposition of triglycerides in hepatocytes.[4] The clinical spectrum of NAFLD ranges from simple steatosis to nonalcoholic steatohepatitis (NASH), a progressive form of CLD resulting in cirrhosis, hepatic failure, and even hepatocellular carcinoma (HCC).[5,6] Prognosis strongly depends on histological severity. Whereas laboratory test abnormalities and radiographic findings may be suggestive of NAFLD, histological evaluation remains the only means of accurately distinguishing NASH from simple steatosis or steatosis with inflammation.[7] Liver biopsy is the recommended reference standard for the diagnosis and staging of fibrosis in NAFLD patients. However, the procedure carries a small risk of complications and may not be acceptable to some patients.[8] Furthermore, because a standard liver biopsy sample represents only approximately 1/50,000th of the whole liver, sampling bias may occur.[9] Moreover, the accuracy of liver biopsy is limited because of intra- and interobserver variability.[10] As such, a noninvasive test for estimation of the fibrosis stage of NAFLD is urgently needed. Several clinical trials have reported use of serum markers and imaging findings by sonographic transient elastography (FibroScan; Echosens, Paris, France)[11] and acoustic radiation

Abbreviations: ALT, alanine aminotransferase; ARFI, acoustic radiation force impulse; AST, aspartate aminotransferase; AUC, area under the curve; AUROC, area under the ROC curve; BMI, body mass index; CHC, chronic hepatitis C; CLD, chronic liver disease; CT, computed tomography; HCC, hepatocellular carcinoma; HVPG, hepatic venous pressure gradient; IR, insulin resistance; NAFLD, nonalcoholic fatty liver diseases; NAS, NAFLD activity score; NASH, nonalcoholic steatohepatitis; NPV, negative predictive value; PH, portal hypertension; PPV, positive predictive value; ROC, receiver operating characteristic; ROI, region of interest; SBI, spleen-body index; SEP, splenic elasticity for PH score; US, ultrasound.

From the [1]Departments of Gastroenterology and Metabology; and [2]Pathogenomics, Ehime University Graduate School of Medicine, Ehime, Japan.

Received December 2, 2011; accepted March 26, 2012.

This study was funded, in part, by a Grant-in-Aid for Scientific Research (JSPS KAKENHI 21590848) from the Japanese Ministry of Education, Culture, Sports, Science and Technology and, in part, by a Grant-in-Aid for Scientific Research and Development from the Japanese Ministry of Health, Labor and Welfare, Japan.

Address reprint requests to: Yoichi Hiasa, M.D., Ph.D., Department of Gastroenterology and Metabology, Ehime University Graduate School of Medicine, Shitsukawa, Toon, Ehime 791-0295, Japan. E-mail: hiasa@m.ehime-u.ac.jp; fax: +81-89-960-5310.

View this article online at wileyonlinelibrary.com.

DOI 10.1002/hep.25756

Potential conflict of interest: Nothing to report.

Additional Supporting Information may be found in the online version of this article.

force impulse (ARFI).[12] Transient elastography is not a real-time technique, because the image is not visible while the measurement is being taken. Reproducibility of FibroScan is also reduced in patients with chronic hepatitis C (CHC).[13] Though ARFI is a useful method for diagnosing advanced fibrosis in patients with NASH, estimation of the early stages of fibrosis is not adequate.[12] Real-time tissue elastography is a relatively new method for the measurement of tissue elasticity.[14] We previously reported the diagnostic efficacy of this technique for liver fibrosis in patients with CHC infection.[15] We also reported that splenic elasticity measured by real-time tissue elastography is significantly related to the hepatic venous pressure gradient (HVPG) and is a predictive marker for the development of gastroesophageal varices.[16]

In this study, we investigated the clinical usefulness of real-time tissue elastography in patients with NAFLD. First, we confirmed the efficacy of real-time tissue elastography for measuring hepatic elasticity in patients with NAFLD. Second, we evaluated the degree of portal hypertension (PH) by measuring splenic elasticity using real-time tissue elastography in patients with NAFLD. To confirm our findings, we evaluated the findings of patients in the training set and applied them to patients in the validation set.

Patients and Methods

Patients. All subjects gave informed consent, and the study was approved by the institutional ethics committee. A total of 187 consecutive patients with NAFLD undergoing liver biopsy at Ehime University Hospital (Ehime, Japan) were enrolled prospectively between January 2009 and February 2012. Of these, 6 patients (4 in the training set and 2 in the validation set) in whom an elastography image could not be obtained as a result of severe obesity were excluded from this study. Hence, 181 eligible patients were divided into two groups. Consecutive patients enrolled from January 2009 to July 2011 constituted the training set to evaluate the stage of hepatic fibrosis (n = 106). Subsequently, to validate the diagnostic accuracy of elastography for hepatic fibrosis, more patients were enrolled between August 2011 and February 2012 as the validation set (n = 75) (Supporting Fig. 1). Clinical and laboratory data were collected at the time of liver biopsy. Patients were excluded if they consumed more than 20 g of alcohol per day or were administered nonselective beta-blockers. Patients with secondary causes of hepatic steatosis (e.g., chronic use of systemic corticosteroids), positive hepatitis B surface antigen, and positive anti–hepatitis C antibody were also excluded. History of autoimmune hepatitis, primary biliary cirrhosis, sclerosing cholangitis, hemochromatosis, alpha 1-antitrypsin deficiency, or Wilson's disease was ruled out. Patients with huge shunts, in which the diameter of the collateral vessels was greater than 10 mm on computed tomography (CT) imaging, were also excluded.

Clinical and Laboratory Assessments. Relevant clinical data, such as sex, age, weight, height, and alcohol intake (g/day), were collected. Body mass index (BMI) was calculated as weight (kg) divided by height (m) squared. Venous blood samples were obtained after patients had fasted overnight (more than 12 hours).

In patients with biochemical data, the results of real-time tissue elastography were compared with that of other prediction scores. HAIR score was calculated by adding scores for the following: hypertension = 1 point; alanine aminotransferase (ALT) >40 (U/L) = 1 point; and insulin resistance (IR) index >5.0 = 1 point.[17] Palekar's score was calculated by summing the risk factors of age ≥50 years, female sex, aspartate aminotransferase (AST) ≥45 (U/L), BMI ≥30 (kg/m^2), AST/ALT ratio, and hyaluronic acid ≥55 (mcg/L).[18] NAFIC score was calculated by summing the following: serum ferritin ≥200 (ng/mL; female) or ≥300 (ng/mL; male) = 1 point; fasting insulin ≥10 (μU/mL) = 1 point; and type IV collagen 7s ≥5.0 (ng/mL) = 2 points.[19] Spleen-body index (SBI) was the maximal CT axial section (cm^2)/body surface area (cm^2) × 10^4.[20] FIB-4 score was calculated as follows: age × AST (U/L)/platelet count (×10^9/L) × $\sqrt{}$ALT (U/L).[21] NAFLD fibrosis score was calculated according to the following formula: −1.675 + 0.037 × age (years) + 0.094 × BMI (kg/m^2) + 1.13 × impaired fasting glycemia or diabetes (yes = 1; no = 0) + 0.99 × AST/ALT ratio − 0.013 × platelet (×10^9/L) − 0.66 × albumin (g/dL).[22] BARD score was the weighted sum of three variables (BMI >28 = 1 point; AST/ALT ratio >0.8 = 2 points; and diabetes = 1 point).[23]

Histological Assessment. Ultrasound (US)-guided percutaneous liver biopsy, using a 1.6-mm-diameter, 150-mm-length needle with suction technique, was performed within 1 week after hospitalization. Liver biopsy samples less than 12 mm long were excluded, because a sampling error for identifying liver fibrosis may occur with such samples.[24] Liver biopsy samples were fixed in formalin and embedded in paraffin. Slices (4 μm thick) were stained with hematoxylin and

eosin and impregnated with silver. Liver biopsies that contained fewer than five portal tracts (except in cases of cirrhosis) were excluded from the histologic analysis. The stage of fibrosis was diagnosed by two pathologists who were blinded to the patients' characteristics (Y.S. and Y.T., with 10 and 13 years of experience, respectively). We used the NASH Clinical Research Network histology scoring system.[25,26] Histological features were grouped into five broad categories: steatosis; inflammation; hepatocellular injury; fibrosis; and miscellaneous features. Fibrosis was staged on a 4-point scale from F0 to F4 as follows: stage 0 = absence of fibrosis; stage 1 = perisinusoidal or periportal fibrosis; stage 2 = combined perisinusoidal and portal/periportal fibrosis; stage 3 = bridging fibrosis; and stage 4 = cirrhosis.

Real-Time Tissue Elastography. Real-time tissue elastography was performed within 3 days before liver biopsy. Hepatic elasticity was measured by using a US scanner, including real-time tissue elastography (EUB-7500; Hitachi Medical Systems, Tokyo, Japan) with a linear probe (EUP-L52; central frequency, 5.5 MHz). This scanner displays the color-coded elastography image overlaid on the B-mode image in real time. The elastic ratio is the ratio of strain distribution in two selected regions of interest (ROIs). The ROI was simultaneously placed on small intrahepatic venous vessels with a diameter of less than 3 mm and on the hepatic parenchyma. Subsequently, the ratio of the value in the intrahepatic venous small vessels was divided by the value in the hepatic parenchyma to generate the elastic ratio (Supporting Fig. 2).[15,16] We previously reported that splenic elasticity, measured by real-time tissue elastography, correlates with HVPG.[16] In our previous study, we demonstrated a correlation between splenic elastic ratio and HVPG ($r = 0.85$; HVPG = splenic elasticity × 1.63-2.88). We called the result of this formula the splenic elasticity for PH (SEP) score.

Measurement of HVPG. We obtained consent for hepatic venography from 8 patients with NAFLD who required hepatic angiography and venography for further examination. These patients were suffering from HCC or complications resulting from PH (e.g., gastroesophageal varices, ascites, edema, or encephalopathy). The right hepatic vein was catheterized through the right femoral vein, and pressure in both the wedged and free positions was measured using a 5-Fr balloon-tipped catheter. The HVPG was calculated by subtracting the free hepatic venous pressure from the wedged venous pressure.

Table 1. Clinical Characteristics and Laboratory Data of Patients

Characteristics	Training Set	Validation Set	All Sets
N	106	75	181
Female/male	54/52	41/34	95/86
Age	56.0 ± 14.1	62.5 ± 15.3	58.1 ± 15.0
BMI (kg/m^2)	27.3 ± 5.7	25.3 ± 6.0	26.5 ± 5.9
AST (U/L)	43.0 ± 31.0	52.0 ± 48.9	46.7 ± 39.4
ALT (U/L)	53.3 ± 52.5	60.7 ± 72.8	56.3 ± 61.4
GGT (U/L)	60.6 ± 80.3	93.7 ± 184.9	73.8 ± 132.9
ALB (g/dL)	4.1 ± 0.5	3.9 ± 0.6	4.0 ± 0.5
Platelet counts (×10^4/mL)	20.8 ± 7.2	19.3 ± 6.3	20.2 ± 6.8
FBS (mg/dL)	126.5 ± 52.5	122.6 ± 47.6	125.0 ± 50.4
IRI (μU/mL)	17.8 ± 26.6	4.6 ± 4.9	17.7 ± 24.3
HOMA-IR	5.4 ± 8.1	4.3 ± 3.8	5.1 ± 7.0
Hyaluronic acid (ng/dL)	83.9 ± 121.4	170.9 ± 377.9	116.4 ± 252.5
Uric acid (mg/dL)	5.8 ± 1.6	5.9 ± 1.6	5.9 ± 1.6
Cholesterol (mg/dL)	197.2 ± 41.7	197.3 ± 43.6	197.3 ± 42.4
Triglycerides (mg/dL)	144.0 ± 83.5	129.2 ± 106.0	136.9 ± 75.5
LDL cholesterol (mg/dL)	120.5 ± 36.5	129.9 ± 106.1	124.1 ± 73.4

Abbreviations: GGT, gamma-glutamyl transferase; ALB, albumin; FBS, fetal bovine serum; IRI, insulin resistance index; HOMA-IR, homeostasis model of insulin resistance; LDL, low-density lipoprotein.

Statistical Analysis. Results are expressed as mean ± standard deviations. Data were analyzed by using the Student t test for unpaired data and the chi-square test and Fisher's exact test, as appropriate. Receiver operating characteristic (ROC) curves were constructed, and the area under the ROC curve (AUROC) was calculated by the trapezoidal rule. Optimal cut-off values for liver stiffness were selected to maximize sensitivity, specificity, and diagnostic accuracy. Sensitivity, specificity, positive predictive value (PPV), and negative predictive value (NPV) were calculated by using cutoffs obtained by ROC curves. Multiple regression modeling was used to identify histological factors that correlated with elastic ratio. All data were analyzed with commercial software (JMP, version 9; SAS Institute Japan, Tokyo, Japan).

Results

Patient Characteristics. The characteristics of the two independent study groups are shown in Table 1. Four patients in the training set and 2 in the validation set were excluded from the study, because their images of real-time tissue elastography could not be displayed as a result of excessive amounts of subcutaneous fat (more than 35 mm). The histological findings of both sets are shown in Table 2.

Accuracy of Real-Time Tissue Elastography. Median elastic ratios in patients with F0, F1, F2, F3, and

Table 2. NASH Clinical Research Network Scoring System Scores in Training and Validation Set

Histology Variable	Training Set (%) (n = 106)	Validation Set (%) (n = 75)	All Sets (%) (n = 181)
Steatosis grade			
0: <5%	0	0	0
1: 5%-33%	59 (56)	51 (68)	110 (60.8)
2: 34%-66%	32 (30)	17 (23)	49 (27.1)
3: >66%	15 (14)	7 (9)	22 (12.1)
Steatosis location			
0: zone 3	69 (65)	42 (56)	111 (61.3)
1: zone 1	2 (2)	1 (1)	3 (1.7)
2: azonal	19 (18)	15 (20)	34 (18.8)
3: panancinar	16 (15)	17 (23)	33 (18.2)
Microvesicular steatosis			
0: not present	98 (92)	66 (88)	164 (91)
1: present	8 (8)	9 (12)	17 (9)
Fibrosis stage			
0	34 (32)	42 (56)	76 (42)
1A	10 (9)	2 (6)	12 (7)
1B	5 (5)	2 (6)	7 (4)
1C	6 (6)	2 (6)	8 (4)
2	18 (17)	9 (12)	27 (15)
3	20 (19)	7 (9)	27 (15)
4	13 (12)	11 (14)	24 (13)
Lobular inflammation			
0: none	32 (30)	35 (47)	67 (37)
1: <2	49 (46)	30 (40)	79 (44)
2: 2-4	23 (22)	9 (12)	32 (18)
3: >4	2 (2)	1 (1)	3 (2)
Macrogranulomus			
0: absent	67 (63)	56 (75)	123 (68)
1: present	39 (37)	19 (25)	58 (32)
Large lipogranulomus			
0: absent	74 (70)	58 (77)	132 (73)
1: present	32 (30)	17 (23)	58 (27)
Portal inflammation			
0: none to minimal	81 (76)	63 (84)	144 (80)
1: greater than minimal	25 (24)	12 (16)	37 (20)
Ballooning			
0: none	47 (44)	43 (57)	90 (50)
1: few	38 (36)	23 (31)	61 (34)
2: many	21 (20)	9 (12)	30 (16)
Acidophil bodies			
0: none to rare	100 (94)	74 (99)	174 (96)
1: many	6 (6)	1 (1)	7 (4)
Pigmented macrophages			
0: none to rare	99 (93)	72 (96)	171 (94)
1: many	7 (7)	3 (4)	10 (6)
Megamitochondria			
0: none to rare	99 (93)	71 (75)	170 (94)
1: many	7 (7)	4 (5)	11 (6)
Mallory's hyaline			
0: none to rare	93 (88)	67 (89)	160 (88)
1: many	13 (12)	8 (11)	21 (12)
Glycogenated nuclei			
0: none to rare	53 (50)	39 (52)	92 (51)
1: many	53 (50)	36 (48)	89 (49)
Diagnostic classification			
0: not steatohepatitis	34 (21)	36 (48)	70 (39)
1: possible/borderline	22 (32)	15 (20)	37 (20)
2: definite steatohepatitis	50 (47)	24 (32)	74 (41)

Values are N (%).

F4 disease in the training cohort were 2.1, 2.4, 2.7, 3.5, and 4.3, respectively, demonstrating a stepwise increase with increasing severity of hepatic fibrosis ($P < 0.0001$) (Fig. 1A). Median elastic ratios with NAFLD activity scores (NAS) less than 4 and more than 5 were 2.3 and 2.9, respectively ($P = 0.0016$) (Fig. 1B) in the training cohort. The accuracy of real-time tissue elastography in detecting F1 or higher, F2 or higher, F3 or higher, and F4 stages was 0.838, 0.853, 0.878, and 0.965, respectively, based on calculation of the AUROC curve.

In the training set, the best elastic ratio cutoff for F2 or greater stage was 2.67 (Table 3). The NPV to exclude F2 or greater stage was 82.5%. Sensitivity and specificity to rule out or rule in F2 disease were high, being 86.0% and 88.6%, respectively. The optimal cut-off for F3 or greater stage was 3.02 (Table 3). Both sensitivity and specificity were very high, being 88.2% and 91.5%, respectively. The NPV to exclude advanced fibrosis (i.e., greater than F3 stage) was 94.2%. The best cutoff for F4 stage was 3.36. Both sensitivity and specificity were extremely high, being 100% and 85.6%, respectively. The NPV for liver cirrhosis was 100%. In the validation set, assessment of diagnostic accuracy for each fibrosis stage was performed by using the cut-off values from the training set. The NPV to exclude F2 or greater stage was 95.7%. Both sensitivity and specificity were extremely high, at 92.3% and 89.8%, respectively. The NPV to exclude F3 or greater stage was 96.5%. Both sensitivity and specificity were extremely high, being 88.9% and 96.5%, respectively. The NPV to exclude F4 or greater stage was 100%. Both sensitivity and specificity were extremely high, at 100% and 95.3%, respectively (Table 3).

Correlation Between Hepatic Elastic Ratio and Each Histological Parameter. The predictive value for each histological parameter was analyzed (Table 4). Because the best hepatic elastic ratio cutoff for F2 or greater stage was 2.67, we analyzed each histological parameter for a hepatic elastic ratio >2.67. Perivenular fibrosis ($P < 0.0001$), pericellular fibrosis ($P < 0.0001$), portal fibrosis ($P < 0.0001$), bridging fibrosis ($P < 0.0001$), lobular inflammation ($P < 0.0001$), hepatocellular ballooning ($P = 0.0200$), Mallory body ($P = 0.0040$), and portal inflammation ($P < 0.0001$) were significant predictors for elastic ratio by univariate regression analysis. These factors were analyzed by multiple regression modeling, which revealed portal fibrosis as the only independent factor for predicting elastic ratio (Table 4).

Comparison Between AUROC Curve, Calculated by Real-Time Tissue Elastography and Other Scoring Systems. The area under the curve (AUC) for

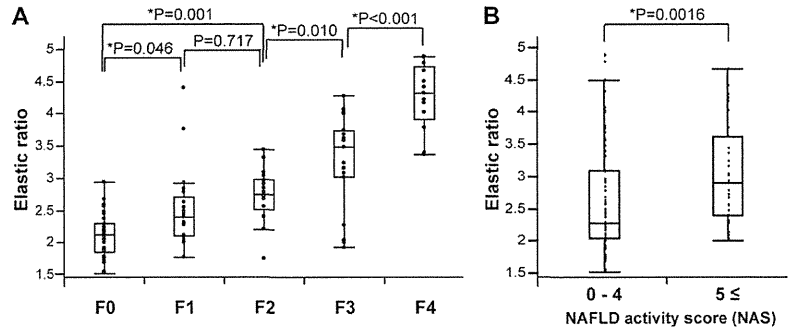

Fig. 1. (A) Hepatic elastic ratio for each NAFLD fibrosis stage. The vertical axis is a logarithmic scale. Tops and bottoms of the boxes = 1st and 3rd quartiles. The length of the box represents the interquartile range within which 50% of the values are located. F1 versus F2 was not significantly different (P = 0.717), whereas all other combinations were significantly different. (B) Hepatic elastic ratio for each NAS. The median elastic ratios with NAS more than 5 were significantly high (P = 0.0016).

predicting each fibrosis stage is shown in Table 5. HAIR, Palekar's score, NAFIC, and SBI are scoring systems for diagnosing early stages of NASH. Hepatic elastic ratio was the most useful score for differentiating F0 versus F1-F4 and F0-F1 versus F2-F4. Platelet count, FIB-4, NASH fibrosis score, and BARD score are reportedly useful for the diagnosis of advanced fibrosis in NASH. In our study, hepatic elastic ratio was the most useful approach for differentiating F0-F2 versus F3-F4 and F0-F3 versus F4 disease and in diagnosing patients with advanced fibrosis (Table 5; Supporting Fig. 3).

Correlation Between SEP Score and Each Histological Parameter. We evaluated the correlation between SEP score and HVPG in the 8 patients who gave consent to be examined with hepatic venography. SEP score was observed to significantly correlate with HVPG in patients with NAFLD (r = 0.91; P = 0.002). This result is similar to the data that we previously reported in patients with hepatitis C[16] (Supporting Fig. 4). HVPG greater than 6 mmHg is considered PH.[27] In our previous study, an HVPG of 6 mmHg corresponded with a SEP score of 6.[16] Therefore, we analyzed predictive factors associated with a SEP score of >6. Data from univariate and multivariate analyses are shown in Table 6. Perivenular fibrosis (P < 0.001), pericellular fibrosis (P = 0.001), portal fibrosis (P = 0.001), bridging fibrosis (P < 0.001), lobular inflammation (P = 0.039), hepatocellular ballooning (P = 0.088), Mallory body (P = 0.266), and portal inflammation (P = 0.003) were significant predictors for elastic ratio by univariate regression analysis. However, when these factors were analyzed by multiple regression modeling, no independent factors for predicting elastic ratio were revealed (Table 6). Perivenular fibrosis and portal inflammation tended to correlate with SEP score, though the tendency was not statistically significant.

Association Between SEP Score and Portal and Arterial Blood Flow and Hepatic Elasticity in NAFLD. We examined portal and hepatic arterial blood flow in patients with NAFLD and analyzed their association with SEP score, because these flows would be influenced by PH. The change of hepatic blood flow is shown in Fig. 2. As SEP score increased, maximum portal blood flow diminished. By contrast, maximum blood flow in the hepatic artery increased with increasing SEP score. These data confirm that SEP score was reflective of PH, and that SEP score would be a useful predictive factor for PH in patients with NAFLD. SEP scores in each fibrosis stage are shown in Supporting Fig. 5. Mild elevation of SEP score (between 6 and 10) existed in F2, F3, and F4 stages. Severe elevation of SEP score (>10) existed only in F4 stage, indicating that although severe PH is only observed in patients with cirrhosis, PH can also occur in patients with milder stages of fibrosis (Supporting Fig. 5).

Table 3. Sensitivity, Specificity, PPV, NPV, and Diagnostic Accuracy of Cut-Off Values for Hepatic Elasticity in Predicting the Presence of Hepatic Fibrosis

Patient Group and Cut-Off Value		Sensitivity (%)	Specificity (%)	PPV (%)	NPV (%)	Diagnostic Accuracy (%)
F0 versus F1-F4	Training set	64.9 (48/74)	96.9 (31/32)	98.0 (48/49)	54.4 (31/57)	74.5 (79/106)
2.47	Validation set	75.0 (24/32)	88.4 (38/43)	82.8 (24/29)	82.6 (38/46)	82.6 (62/75)
F0-F1 versus F2-F4	Training set	86.0 (43/50)	88.6 (47/53)	87.8 (43/49)	82.5 (47/57)	84.9 (97/106)
2.67	Validation set	92.3 (24/26)	89.8 (44/49)	82.8 (24/29)	95.7 (44/46)	92.3 (24/26)
F0-F2 versus F3-F4	Training set	88.2 (30/34)	91.5 (65/71)	83.3 (30/36)	94.2 (65/6)	89.6 (95/106)
3.02	Validation set	88.9 (16/18)	96.5 (55/57)	88.9 (16/18)	96.5 (55/57)	94.7 (71/75)
F0-F3 versus F4	Training set	100 (16/16)	85.6 (77/90)	55.2 (16/29)	100 (77/77)	87.7 (93/106)
3.36	Validation set	100 (11/11)	95.3 (61/64)	78.6 (11/14)	100 (61/61)	96.0 (72/75)

Table 4. The Predictive Factor for Hepatic Elasticity More Than 2.67 by Univariate and Multivariate Regression Model

	Univariate Analysis		Multivariate Analysis	
Parameter	OR (95% CI)	P Value	OR (95% CI)	P Value
Perivenular fibrosis*	21.47 (8.14-63.33)	<0.001	3.28 (0.40-30.23)	0.203
Pericellular fibrosis*	15.58 (5.43-56.94)	<0.001	1.58 (0.10-23.73)	0.704
Portal fibrosis†	33.60 (12.03-109.39)	<0.001	11.60 (2.13-86.26)	0.005
Bridging fibrosis*	17.35 (5.94-64.23)	<0.001	1.78 (0.12-46.32)	0.671
Steatosis	1.71 (0.16-37.79)	0.662		
Lobular inflammation*	23.33 (4.10-442.16)	<0.001	7.24 (0.14-74.06)	0.583
Hepatocellular ballooning*	4.13 (1.31-14.80)	0.020	1.34 (0.08-29.30)	0.837
Mallory body*	7.70 (1.56-52.64)	0.004	3.40 (0.43-38.14)	0.254
Portal inflammation*	10.21 (3.18-40.45)	<0.001	8.76 (0.98-11.09)	0.052

Abbreviations: OR, odds ratio; 95% CI, 95% confidence interval.
*Significant factor by univariate analysis.
†Significant factor by both univariate and multivariate analysis.

Discussion

In this study, we found that liver stiffness measured by real-time tissue elastography is a useful predictive factor for diagnosis of the stage of fibrosis in patients with NAFLD. Additionally, by using the SEP score, we showed that PH could exist even in the F2 fibrosis stage in patients with NAFLD. However, severe PH (SEP score >10) was only found among patients with stage F4 fibrosis.

We evaluated which histological factors correlated with hepatic elastic ratio in NAFLD patients in our study. Using multivariate analysis, we found that only portal fibrosis significantly correlated with increased hepatic elastic ratio measured by real-time tissue elastography (Table 4). Compared with the NAS score, the hepatic elastic ratio was significantly higher in patients with NAS ≥5, rather than in the group of NAS ≤4 (Fig. 1B). This is likely related to the difference in the amount of fibrosis in both groups. In the low NAS score group, the percentage of patients with F0 stage was high (32 of 71; 45.1%), whereas in the high NAS score group, the percentage was low (2 of 35; 5.7%). Among the histological factors, only portal fibrosis, but not perivenular fibrosis or pericellular fibrosis, was found to be significantly associated with hepatic elasticity through multivariate analysis. The amount of fibrous tissue resulting from the fibrotic changes would be most accurately reflected by the hepatic elastic ratio as determined by real-time tissue elastography, which is reasonable considering the total histological change of liver fibrosis.

Table 5. AUROC Curve of Each Fibrosis Score

	Fibrosis Stage			
Score	≥F1	≥F2	≥F3	F4
Elastic ratio	0.838	0.853	0.878	0.965
HAIR	0.613	0.536	0.500	0.616
Paleker's score	0.710	0.751	0.803	0.803
NAFIC	0.720	0.713	0.739	0.881
SBI	0.592	0.650	0.713	0.782
Platelet count	0.648	0.799	0.856	0.872
Hyaluronic acid	0.679	0.784	0.860	0.959
NASH fibrosis score	0.631	0.793	0.838	0.896
BARD score	0.566	0.671	0.685	0.754
FIB-4	0.751	0.839	0.861	0.908
A/P ratio	0.728	0.819	0.847	0.869

A/P ratio, arterio-portal ratio.

Several previous reports have focused on the differential diagnosis of simple steatosis versus NASH with early fibrosis. HAIR,[17] Palekar's score,[18] NAFIC score,[19] and SBI[20] were reported to be useful scoring systems for diagnosing the early stage of NASH. The ability to diagnose the early stage of NASH is relevant, and these scores have the benefit of being easy to use because they are calculated using laboratory data or spleen volume. However, the hepatic elastic ratio, determined by real-time tissue elastography, is superior to these scoring systems. This is reasonable because the scoring systems reported previously were developed by multivariate analysis with indirect parameters, whereas the hepatic elastic ratio, by real-time tissue elastography, is determined from direct evaluation of the liver. In patients with advanced stages of NASH, platelet count, NASH fibrosis score,[22] BARD score,[23] and FIB-4[21] were reported to be useful markers. However, we found that the AUC of the hepatic elastic ratio is superior to these scoring systems. In both the advanced and early stages of NASH, the hepatic elastic ratio measured by real-time tissue elastography could be one of the most useful diagnostic methods. For the distinction between F0 and ≥F1 stage, the specificity and PPV of the hepatic elastic ratio were more than 90% (Table 3). Furthermore, for distinguishing each F stage among patients with ≥F2 disease, sensitivity, specificity, PPV, and NPV were all greater than 80% (Table 3).

Table 6. The Predictive Factor for SEP Score More Than 6.00 by Univariate and Multivariate Regression Model

	Univariate Analysis		Multivariate Analysis	
Parameter	OR (95% CI)	*P* Value	OR (95% CI)	*P* Value
Perivenular fibrosis*	10.20 (3.68-33.48)	<0.001	5.20 (0.96-37.03)	0.069
Pericellular fibrosis*	11.85 (3.24-76.70)	0.001	3.10 (0.34-68.04)	0.356
Portal fibrosis*	4.92 (1.95-13.77)	0.001	2.30 (0.38-17.28)	0.382
Bridging fibrosis*	8.05 (3.16-21.75)	<0.001	3.75 (0.71-23.45)	0.129
Steatosis	5.41 (0.49-120.86)	0.179		
Lobular inflammation*	6.17 (1.08-116.87)	0.039	1.29 (0.05-16.23)	0.851
Hepatocellular ballooning	3.98 (0.96-27.18)	0.088		
Mallory body	2.05 (0.54-7.22)	0.266		
Portal inflammation*	5.67 (1.85-19.24)	0.003	4.06 (0.99-18.53)	0.056

Abbreviations: OR, odds ratio; 95% CI, 95% confidence interval.
*Significant factor by univariate analysis.

The box plot shows the difference of median value in each of the early fibrosis stages, and the difference is apparent in our method (Fig. 1A).

We believe ours to be the first study examining PH in patients with NAFLD. We previously reported that splenic elasticity strongly correlated with HVPG.[16] In our previous study, we proposed a marker for PH (the SEP score, which is splenic elasticity × 1.63 − 2.88). Supporting Fig. 5 shows the SEP score in each fibrosis stage and indicates that PH was present even in fibrosis F2 stage in patients with NAFLD. We propose a mechanism for how PH occurs in patients with NASH in such early stages of fibrosis (Supporting Fig. 6). In our study, among the histological factors in patients with NAFLD, portal fibrosis, portal inflammation, pericellular fibrosis, perivenular fibrosis, and bridging fibrosis correlated with the appearance of PH by univariate analysis (Table 6). Among these selected factors, portal inflammation, which would reflect an inflow block from the portal vein to the sinusoidal area, and perivenular fibrosis, which would reflect an outflow block from the sinusoidal area to the hepatic vein, tend to be predictive factors for mild PH (Table 6). These histological changes would result in a decrease in portal blood flow in the liver and an increase in hepatic artery flow.[28] Actually, the changes in hepatic blood flow are obvious in Doppler sonography (Fig. 2). These changes in blood flow would induce PH.[28] PH evokes hyperplasia of splenic histiocytes, arterial terminal lengthening, increased white pulp volume, and fibrosis between splenic trabeculae.[29-32] These changes might result in an increase in splenic elasticity, which is the change that most correlated with PH in our previous study.[16] An increase in splenic elasticity results in an increase in SEP score. Taken together with hepatic elasticity, the SEP score would be useful not only to evaluate PH, but also to detect the early stage of NASH among patients with NAFLD (Supporting Fig. 5).

Our study has some limitations. First, we used needle biopsy of the liver, which creates the possibility of over- or underestimation of histological stage by sampling error. Our inclusion criteria considered the number of portal tracts and the length of specimen to exclude bias. Second, we did not examine imaging methods other than real-time tissue elastography, so we cannot assess superiority among different imaging methods, including transient elastography, ARFI, or magnetic resonance elastography.[12,33] Such a

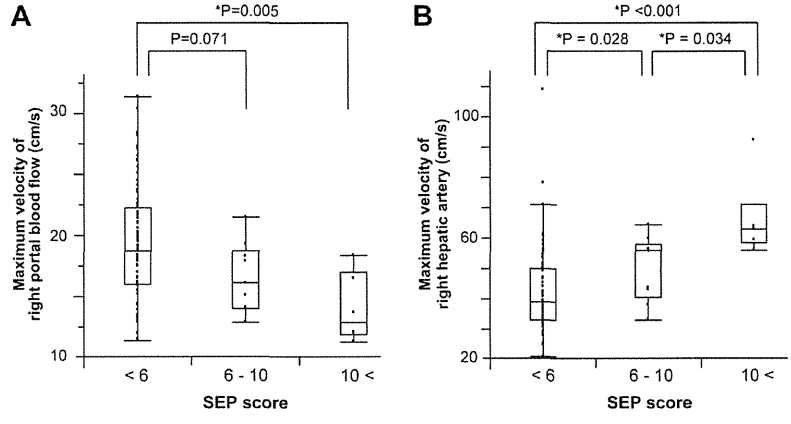

Fig. 2. Maximum velocity of right portal and hepatic artery blood flow for each SEP score. (A) Velocity of portal blood flow was reduced in the elevated SEP score group. (B) Velocity of hepatic artery blood flow was increased in the advanced PH group.

comparison would need to be addressed in a future study. Third, we could get consent to perform hepatic venography and assess the HVPG in only 8 patients, who presented for the treatment of HCC or for survey of the complications of PH (e.g., gastroesophageal varices, ascites, edema, or encephalopathy). We had ethical reservations regarding performing hepatic venography for all the enrolled patients with NAFLD, because it would mean an invasive study in a population without serious fibrosis or cirrhosis or HCC. Yet, the data from the 8 patients indicated a significant correlation between HVPG and SEP scores, which is similar to our previously reported results from patients with hepatitis C.[16] We substituted the SEP score, which was identified by real-time tissue elastography, for the HVPG. Real-time tissue elastography is noninvasive, so patients with NAFLD were more amenable to enrollment in the study, and we could conduct evaluations on an outpatient basis.

In conclusion, real-time tissue elastography reliably identified the early stage of fibrosis in patients with NAFLD. Thus, it could be a useful tool for evaluating hepatic fibrosis as well as PH in these patients.

References

1. Bellentani S, Saccoccio G, Masutti F, Crocè LS, Brandi G, Sasso F, et al. Prevalence of and risk factors for hepatic steatosis in Northern Italy. Ann Intern Med 2000;132:112-117.
2. Marchesini G, Bugianesi E, Forlani G, Cerrelli F, Lenzi M, Manini R, et al. Nonalcoholic fatty liver, steatohepatitis, and the metabolic syndrome. HEPATOLOGY 2003;37:917-923.
3. Fan JG, Zhu J, Li XJ, Chen L, Li L, Dai F, et al. Prevalence of and risk factors for fatty liver in a general population of Shanghai, China. J Hepatol 2005;43:508-514.
4. Hui AY, Wong VW, Chan HL, Liew CT, Chan JL, Chan FK, et al. Histological progression of non-alcoholic fatty liver disease in Chinese patients. Aliment Pharmacol Ther 2005;21:407-413.
5. Bugianesi E, Leone N, Vanni E, Marchesini G, Brunello F, Carucci P, et al. Expanding the natural history of nonalcoholic steatohepatitis: from cryptogenic cirrhosis to hepatocellular carcinoma. Gastroenterology 2002;123:134-140.
6. Torres DM, Harrison SA. Diagnosis and therapy of nonalcoholic steatohepatitis. Gastroenterology 2008;134:1682-1698.
7. Brunt EM. Nonalcoholic steatohepatitis. Semin Liver Dis 2004;24:3-20.
8. Al Knawy B, Shiffman M. Percutaneous liver biopsy in clinical practice. Liver Int 2007;27:1166-1173.
9. Ratziu V, Charlotte F, Heurtier A, Gombert S, Giral P, Bruckert E, et al. Sampling variability of liver biopsy in nonalcoholic fatty liver disease. Gastroenterology 2005;128:1898-1906.
10. Rousselet MC, Michalak S, Dupré F, Croué A, Bedossa P, Saint-André JP, et al. Sources of variability in histological scoring of chronic viral hepatitis. HEPATOLOGY 2005;41:257-264.
11. Wong VW, Vergniol J, Wong GL, Foucher J, Chan HL, Le Bail B, et al. Diagnosis of fibrosis and cirrhosis using liver stiffness measurement in nonalcoholic fatty liver disease. HEPATOLOGY 2010;51:454-462.
12. Yoneda M, Suzuki K, Kato S, Fujita K, Nozaki Y, Hosono K, et al. Nonalcoholic fatty liver disease: US-based acoustic radiation force impulse elastography. Radiology 2010;256:640-647.
13. Fraquelli M, Rigamonti C, Casazza G, Conte D, Donato MF, Ronchi G, et al. Reproducibility of transient elastography in the evaluation of liver fibrosis in patients with chronic liver disease. Gut 2007;56:968-973.
14. Friedrich-Rust M, Ong MF, Herrmann E, Dries V, Samaras P, Zeuzem S, et al. Real-time elastography for noninvasive assessment of liver fibrosis in chronic viral hepatitis. AJR Am J Roentgenol 2007;188:758-764.
15. Koizumi Y, Hirooka M, Kisaka Y, Konishi I, Abe M, Murakami H, et al. Liver fibrosis in patients with chronic hepatitis C: noninvasive diagnosis by means of real-time tissue elastography—establishment of the method for measurement. Radiology 2011;258:610-617.
16. Hirooka M, Ochi H, Koizumi Y, Kisaka Y, Abe M, Ikeda Y, et al. Splenic elasticity measured with real-time tissue elastography is a marker of portal hypertension. Radiology 2011;261:960-968.
17. Wai CT, Greenson JK, Fontana RJ, Kalbfleisch JD, Marrero JA, Conjeevaram HS, et al. A simple noninvasive index can predict both significant fibrosis and cirrhosis in patients with chronic hepatitis C. HEPATOLOGY 2003;38:518-526.
18. Palekar NA, Naus R, Larson SP, Ward J, Harrison SA. Clinical model for distinguishing nonalcoholic steatohepatitis from simple steatosis in patients with nonalcoholic fatty liver disease. Liver Int 2006;26:151-156.
19. Sumida Y, Yoneda M, Hyogo H, Yamaguchi K, Ono M, Fujii H, et al. A simple clinical scoring system using ferritin, fasting insulin, and type IV collagen 7S for predicting steatohepatitis in nonalcoholic fatty liver disease. J Gastroenterol 2011;46:257-268.
20. Suzuki K, Kirikoshi H, Yoneda M, Mawatari H, Fujita K, Nozaki Y, et al. Measurement of spleen volume is useful for distinguishing between simple steatosis and early-stage non-alcoholic steatohepatitis. Hepatol Res 2010;40:693-700.
21. Vallet-Pichard A, Mallet V, Nalpas B, Verkarre V, Nalpas A, Dhalluin-Venier V, et al. FIB-4: an inexpensive and accurate marker of fibrosis in HCV infection. Comparison with liver biopsy and fibrotest. HEPATOLOGY 2007;46:32-36.
22. Angulo P, Hui JM, Marchesini G, Bugianesi E, George J, Farrell GC, et al. The NAFLD fibrosis score: a noninvasive system that identifies liver fibrosis in patients with NAFLD. HEPATOLOGY 2007;45:846-854.
23. Harrison SA, Oliver D, Arnold HL, Gogia S, Neuschwander-Tetri BA. Development and validation of a simple NAFLD clinical scoring system for identifying patients without advanced disease. Gut 2008;57:1441-1447.
24. Pagliaro L, Rinaldi F, Craxì A, Di Piazza S, Filippazzo G, Gatto G, et al. Percutaneous blind biopsy versus laparoscopy with guided biopsy in diagnosis of cirrhosis. A prospective, randomized trial. Dig Dis Sci 1983;28:39-43.
25. Brunt EM, Kleiner DE, Wilson LA, Belt P, Neuschwander-Tetri BA; NASH Clinical Research Network (CRN). Nonalcoholic fatty liver disease (NAFLD) activity score and the histopathologic diagnosis in NAFLD: distinct clinicopathologic meanings. HEPATOLOGY 2011;53:810-820.
26. Kleiner DE, Brunt EM, Natta MV, Behling C, Contos MJ, Cummings OW, et al. Design and validation of a histological scoring system for nonalcoholic fatty liver disease. HEPATOLOGY 2005;41:1313-1321.
27. de Franchis R. Evolving consensus in portal hypertension: report of the Baveno IV consensus workshop on methodology of diagnosis and therapy in portal hypertension. J Hepatol 2005;43:167-176.
28. Hirata M, Akbar SM, Horiike N, Onji M. Noninvasive diagnosis of the degree of hepatic fibrosis using ultrasonography in patients with chronic liver disease due to hepatitis C virus. Eur J Clin Invest 2001;31:528-535.
29. Manenti A, Botticelli A, Gibertini G, Botticelli L. Experimental congestive splenomegaly: histological observations in the rat. Pathologica 1993;85:721-724.
30. Cavalli G, Re G, Casali AM. Red pulp arterial terminals in congestive splenomegaly: a morphometric study. Pathol Res Pract 1984;178:590-594.
31. Re G, Casali AM, Cavalli D, Guida G, Cau R, Cavalli G. Histometric analysis of white pulp arterial vessels in congestive splenomegaly. Appl Pathol 1986;4:98-103.
32. Terayama N, Makimoto KP, Kobayashi S, Nakanuma Y, Sasaki M, Saito K, et al. Pathology of the spleen in primary biliary cirrhosis: an autopsy study. Pathol Int 1994;44:753-758.
33. Chen J, Talwalkar JA, Yin M, Glaser KJ, Sanderson SO, Ehman RL. Early detection of nonalcoholic steatohepatitis in patients with nonalcoholic fatty liver disease by using MR elastography. Radiology 2011;259:749-756.

SCIENTIFIC REPORTS

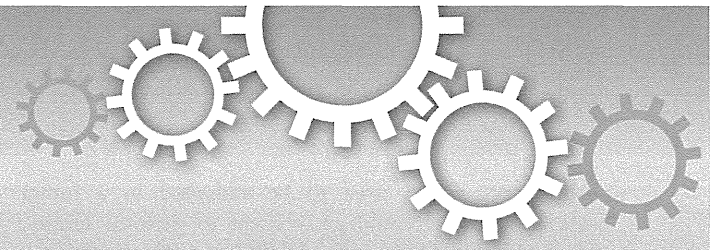

OPEN

SUBJECT AREAS:
GLYCOBIOLOGY
BIOCHEMICAL ASSAYS
ASSAY SYSTEMS
ELISA

Received
3 September 2012

Accepted
27 December 2012

Published
15 January 2013

Correspondence and requests for materials should be addressed to H.N. (h.narimatsu@aist.go.jp)

* These authors contributed equally to this study.

A serum "sweet-doughnut" protein facilitates fibrosis evaluation and therapy assessment in patients with viral hepatitis

Atsushi Kuno[1]*, Yuzuru Ikehara[1]*, Yasuhito Tanaka[2], Kiyoaki Ito[3], Atsushi Matsuda[1], Satoru Sekiya[1], Shuhei Hige[4], Michiie Sakamoto[5], Masayoshi Kage[6], Masashi Mizokami[3] & Hisashi Narimatsu[1]

[1]Research Center for Medical Glycoscience (RCMG), National Institute of Advanced Industrial Science and Technology (AIST), Tsukuba, Japan, [2]Department of Virology & Liver Unit, Nagoya City University Graduate School of Medical Sciences, Nagoya, Japan, [3]The Research Center for Hepatitis and Immunology, National Center for Global Health and Medicine, Ichikawa, Japan, [4]Department of Internal Medicine, Hokkaido University Graduate School of Medicine, Sapporo, Japan, [5]Department of Pathology, School of Medicine, Keio University, Tokyo, Japan, [6]Department of Pathology, Kurume University School of Medicine, Kurume, Japan.

Although liver fibrosis reflects disease severity in chronic hepatitis patients, there has been no simple and accurate system to evaluate the therapeutic effect based on fibrosis. We developed a glycan-based immunoassay, FastLec-Hepa, to fill this unmet need. FastLec-Hepa automatically detects unique fibrosis-related glyco-alteration in serum hyperglycosylated Mac-2 binding protein within 20 min. The serum FastLec-Hepa counts increased with advancing fibrosis and illustrated significant differences in medians between all fibrosis stages. FastLec-Hepa is sufficiently sensitive and quantitative to evaluate the effects of PEG-interferon-α/ribavirin therapy in a short post-therapeutic interval. The obtained fibrosis progression is equivalent to -0.30 stages/year in patients with sustained virological response, and 0.01 stages/year in relapse/nonresponders. Furthermore, long-term follow-up of the severely affected patients found hepatocellular carcinoma developed in patients after therapy whose FastLec-Hepa counts remained above a designated cutoff value. FastLec-Hepa is the only assay currently available for clinically beneficial therapy evaluation through quantitation of disease severity.

The World Health Organization has estimated that the prevalence of chronic infections with hepatitis B virus (HBV) and hepatitis C virus (HCV) is more than 5% of the world population. The high rate of viral transmission worldwide has also resulted in an explosive increase in incidence of liver cirrhosis (LC), because liver fibrosis caused by the persistent infections with HBV and HCV irreversibly progresses in chronic hepatitis (CH) patients without effective treatment. As the incidence of hepatocellular carcinoma (HCC) increases proportionally to the severity of hepatitis and the presence of LC, it is now clear that about 90% of HCC cases originate from infection with HBV or HCV. It is estimated that more than one million patients worldwide die from liver disease related to HBV or HCV infection each year. Immunomodulatory therapy with PEG-interferon-α and ribavirin is the standard treatment for patients with chronic hepatitis C (CHC)[1]. Recent genome-wide association studies have revealed that variation in the host interleukin-28B gene can predict the outcome of therapies for viral clearance[2–4]. Such pharmacokinetic understanding should allow for more precise treatment protocols and follow-up analyses to optimize the opportunity for patients to achieve sustained virological response (SVR)[5,6]. Linear peptidomimetic HCV and NS3/4A serine protease inhibitors such as telaprevir and boceprevir are new drugs that, in combination with PEG-interferon-α and ribavirin, substantially improve the rates of response among patients with HCV genotype 1 infection[1]. Alternatively, suppression of hepatic decompensation in chronic hepatitis B patients with advanced fibrosis and cirrhosis has been evaluated during long-term treatment with antiviral agents, such as adefovir, lamivudine, entecavir, and tenofovir[7]. For example, cumulative entecavir therapy (for at least 3 years) resulted in substantial histological improvement and regression of fibrosis or cirrhosis[8].

The efficacy of therapy is currently evaluated by frequent monitoring of "viral load" or "liver injury"[5]. From the viewpoint of developing preventive strategies for HCC, the risk of HCC development should also be estimated along with them. For this purpose, liver biopsy is generally considered as the gold standard in which fibrosis is subclassified into 5 stages of severity (F0–4). However, this procedure is invasive and shown to cause a high rate of sampling error (about 15% false-negatives for cirrhosis) in patients with diffuse parenchymal liver diseases.

Furthermore, in a retrospective cohort study[9], the rate of fibrosis progression was estimated at about −0.28 stages/year in patients with SVR and 0.02 stages/year in patients with nonsustained virological response (NVR). This indicates that the biopsy is not suitable for evaluating the effect of therapy after a short interval. The procedure has further disadvantages such as inaccuracy, biopsy-related complications, the need for hospitalization, the time involved, and low cost-effectiveness[10]. Therefore, alternative noninvasive assays are desired and should provide a quantifiable readout of fibrosis progression using a method that is accurate, cost-effective and relatively simple.

To date, several methods have been developed[10] including FibroScan, which measures hepatic fibrosis biomechanically as tissue stiffness based on transient elastography. FibroScan has the advantages of being rapid and technically simple; however, its diagnostic success rate is affected by operator skill. Therefore, it has been suggested that FibroScan, in conjunction with assay of serum fibrosis biomarkers, should improve diagnostic accuracy. FibroTest[11] and FibroMeter[12], believed to be the most reliable indices of fibrosis, have been used in the combination assay aiming to eliminate the need for liver biopsy[13,14]. However, FibroTest and FibroMeter do not complement FibroScan in the development of a rapid "on-site diagnosis" system. This is because each requires both extensive and specialized blood analyses (FibroTest requires α2-macroglobulin, apolipoprotein A1, haptoglobin, γ-glutamyltransferase and total bilirubin whereas FibroMeter requires platelet count, prothrombin index, AST, α2-macroglobulin, hyaluronic acid and urea). In addition, both tests require data on age, and also sex for FibroTest.

Glycans are referred to as the face of cells, which reflect their status such as differentiation stage rather than their state of damage, and therefore they can be great markers for chronic disease. In the case of hepatitis, glycans are considered to reflect more specifically the progression of fibrosis than viral load. In the search for a simple and rapid method that is not markedly affected by tissue inflammation and ALT fluctuation, the possibility of glycomic and glycoproteomic techniques has emerged[15,16], and there are reports of some successful examples applicable for use in the clinical laboratories[17–19]. However, the current glycomic techniques require at least 3 hours of sample preparation for analysis and this has markedly reduced the combination use of glycan-based immunoassays with FibroScan. In this report, we describe for the first time, a rapid and simple glycan-based immunoassay, FastLec-Hepa, that can quantify fibrosis as precisely as FibroTest and also readily evaluate the antifibrotic effects of therapy at the clinical site (**Supplementary Fig. 1**). Moreover, we introduce a novel method for rational selection of the "non-fucose binding type" lectins and provide details of how this concept can be adopted for future development of clinically useful glycodiagnostic tools.

Results

Changes in the *N*-glycosylation of M2BP during progression of liver disease. Based on previous reports[20–23], we adopted the serum 90 K/Mac-2 binding protein (M2BP) as a glycoprotein biomarker for liver fibrosis. M2BP is secreted from many cell types, including hepatocytes (http://www.proteinatlas.org/ENSG00000108679), and it has been shown to modulate many processes, particularly those related to cell adhesion. For example, the interaction of M2BP with matrix fibronectin can modulate adhesion and the high expression of M2BP by tumor cells increases the level in the circulation of affected patients. A prominent feature of native human M2BP is its oligomerization to large ring structures[20], resembling a "sugar-powdered doughnut" which is potentially covered with 70–112 *N*-glycans (**Fig. 1a**). To confirm serum M2BP as a valid marker, we performed a pull-down assay with serum (2 μl each) from five individuals in each of the following groups: HCC, LC, CHC or healthy volunteer with normal liver (HV). Although two bands appeared in all HVs and two CHC patients, M2BPs from patients with relatively severe fibrosis, i.e., LC and HCC, migrated as a single band, the mobility of which was similar to that of the lower band for HVs (**Fig. 1b**). Significant increases in band intensity with excessive smearing of the bands were seen for most HCC patients. A subsequent investigation of 125 HCV patients with stage-determined fibrosis showed alteration in the quality and quantity of M2BP during the progression of fibrosis (**Fig. 1c**) and apparent alteration in the amount of each band (**Fig. 1d and e**), as described in the previous investigations[22,23]. M2BP has been shown to have multibranching and sialylated *N*-glycans. Moreover, it has been suggested that extension of polylactosamine on M2BP controls its binding to galectin-3, a major binding partner *in vivo*. Sialylation and extension of polylactosamine affect the charge and size of M2BP and this results in altered electrophoretic migration. Accordingly, we speculate that the size heterogeneity of M2BP seen on electrophoresis is due to such alterations in glycosylation. In fact, the difference in the band migration was eliminated by Sialidase A treatment, and the smearing of the bands in HCC was reduced by treatment with *N*-Glycosidase F (**Supplementary Fig. 2**). These results indicated that the altered quality of M2BP during progression of liver disease was due to changes in *N*-glycosylation.

Selection of the optimal lectin for direct measurement of disease-related M2BP. To construct a reliable assay (see **Supplementary Fig. 3**), we needed to identify a lectin probe that could most readily discriminate the altered *N*-glycans of M2BP and specifically binds to them in serum without pretreatment. For this purpose, we added a subtraction process to our recently described microarray-based selection strategy[16] (**Supplementary Fig. 4**). In brief, we first obtained a typical glycan profile for serum M2BPs by averaging the glycan profiles of M2BPs immunoprecipitated from 125 HCV patient sera by the antibody-overlay lectin microarray[16,18,24] (**step 1**). In this step, we selected 27 lectins binding to M2BP from a 45-lectin array (**Supplementary Fig. 5a**). Most of them bound not only to M2BP (ca. 10 μg/ml in serum), but also to other abundant serum glycoproteins, whereas some suggested rather specific binding to M2BP. We designated them as high-noise lectins or high signal-to-noise (S/N) lectins, respectively (**Fig. 2a**). We then selected the candidate lectins for the assay by subtracting the high-noise lectins from the M2BP-binding lectins (**step 2**), using a glycan profile of whole serum (**Supplementary Fig. 5**)[25]. Comparing the profiles for M2BP and whole serum (**Fig. 2b**), we quickly identified 6 lectins with a high S/N ratio. Interestingly, all lectins identifying fucose modification, which is the most well-known glyco-alteration in liver disease (*Pisum sativum* agglutinin (PSA), *Lens culinaris* agglutinin (LCA), *Aspergillus oryzae* lectin (AOL), and *Aleuria aurantia* lectin (AAL)), were high-noise lectins (**Fig. 2b**). After subtraction, we used both the Mann–Whitney *U* test as a nonparametric test, and receiver-operating characteristic (ROC) analysis, to characterize the diagnostic accuracy of the candidate lectins at each stage of fibrosis: significant fibrosis (F2/F3/F4), severe fibrosis (F3/F4) and cirrhosis (F4) (**step 3**). As a result, we found that the diagnostic score of *Wisteria floribunda* agglutinin (WFA) was superior to the other 5 lectins at every fibrosis stage (**Fig. 2c and Supplementary Fig. 6**).

"Proof-of-concept" experiment for direct quantitation of the serum WFA-binding M2BP by sandwich immunoassay. We quantitatively analyzed the WFA-binding M2BPs (WFA^+-M2BP) in serum. Sera, pretreated as described in the **Methods**, were firstly subjected to affinity capture with 20 μl slurry of WFA-coated agarose gel. The eluted fraction was immunoprecipitated with a capturing antibody against M2BP and the product was analyzed by Western blot. The intensity of the "smearing-band" signal for WFA^+-M2BP gradually increased in proportion to the severity of liver fibrosis (**Supplementary Fig. 7**), as indicated by the red line shown in

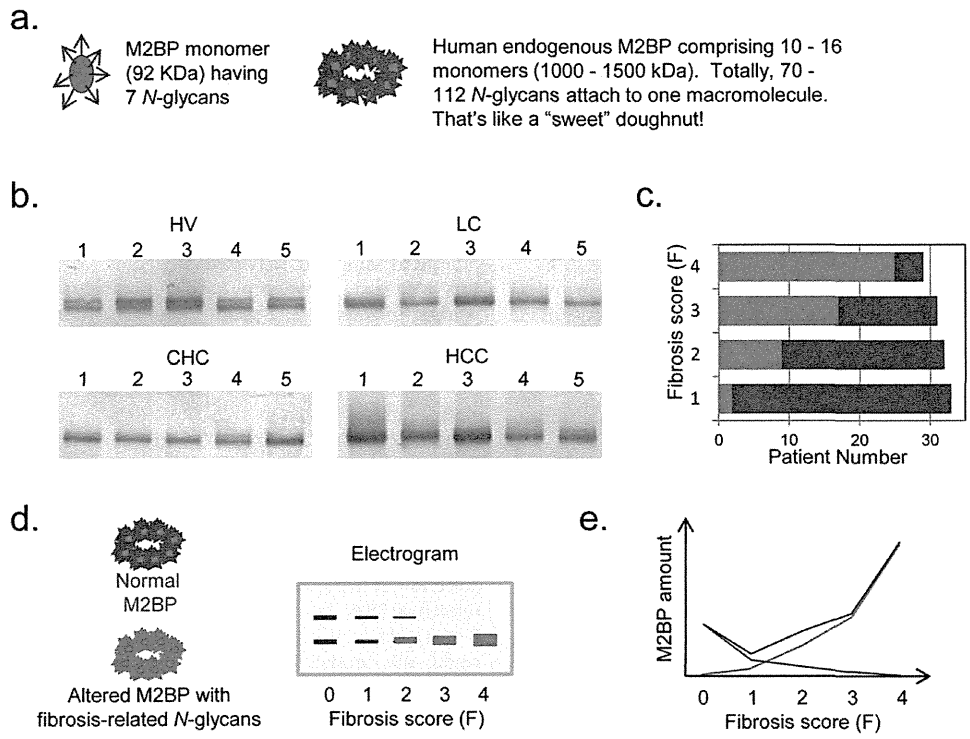

Figure 1 | Changes in the quality and quantity of human serum M2BP with progression of liver fibrosis. (a) The unique shape of human endogenous serum M2BP. The arrowheads and circles represent the *N*-glycan moieties and core protein respectively. (b) Western blot analysis: M2BPs in 2 μl of serum were purified by immunoprecipitation before SDS-PAGE. HV, healthy volunteer; CHC, patient with chronic hepatitis C; LC, HCV-infected patient with liver cirrhosis; and HCC, HCV-infected patient with hepatocellular carcinoma. (c) Number of patients with single (red) or double (blue) band appearance on the blot. The number of bands was determined visually by two independent analysts. The total number of HCV patients who participated in this study was 125 (F0–F1 [$n = 33$], F2 [$n = 32$], F3 [$n = 31$], and F4 [$n = 29$]). (d) Typical changes of serum M2BP band intensities in patients with different fibrosis scores and (e) concentrations based on a previous report on quantitation of serum M2BP by Cheung *et al*[23]. and our present results. The blue bands on the electrogram and blue line on the graph represent M2BPs secreted from normal liver. The red bands and line represent altered M2BP, the concentration of which is suggested to increase with the progression of fibrosis. The black line represents the total concentration of serum M2BP.

Fig. 1e. We next conducted a sandwich immunoassay with WFA and anti-M2BP antibody (see **Supplementary Fig. 3b**). WFA was immobilized on the surface of a 96-well microtiter plate through biotin–streptavidin interaction. We performed the first assay for the WFA-binding activity using recombinant human M2BP (rhM2BP). As a result, a linear regression analysis revealed a linear range of detection from 0.039 to 0.625 μg/ml (**Supplementary Fig. 8a**). Subsequently, we used culture supernatant of a hepatoblastoma cell line HepG2, which expresses WFA^+-M2BP, to illustrate the dose-dependency of the interaction of WFA with M2BP/HepG2. We also showed that heat treatment of the culture supernatant eliminated this binding activity (**Supplementary Fig. 8b**). Finally, we performed a sandwich immunoassay for direct measurement of WFA^+-M2BP in untreated serum samples, and the results correlated well with the quantitative assay using affinity capture and lectin microarray analysis (**Supplementary Fig. 7 and 9**).

FastLec-Hepa: a fully automated sandwich immunoassay for direct quantitation of serum WFA^+-M2BP. We adapted the WFA-antibody immunoassay to the HISCL-2000i bedside clinical chemistry analyzer[18]. We successfully adjusted every reaction condition during the automatic assay by HISCL, which is about a 17-min manipulation. Heat pretreatment of the serum was avoided to ensure both binding avidity and the fast association rate. Repeatability was assessed by performing 10 independent assays of three samples, and the coefficient of variation ranged between 2.1% and 2.5% (data not shown). Sensitivity was determined by triplicate assays of samples generated by 2-fold serial dilution of 50 μg/ml rhM2BP. The linear regression analysis identified a linear range of detection ($R^2 = 1.00$) from 0.025 to 12.5 μg/ml (**Fig. 3a**, a range of 0.025 to 1.6 μg/ml also shown in **Fig. 3b**). The resulting dynamic range was 25-fold that of the manual sandwich immunoassay described above. We next examined whether the HISCL measurements made on serum from HCV patients ($n = 125$) were consistent with lectin microarray analysis, and this comparison resulted in sufficient linearity with coefficient of determination, $R^2 = 0.848$ (**Fig. 3c**). Accordingly, we could perform automatic quantitation of serum WFA^+-M2BP in 180 patients in 1 hour and we have therefore named it FastLec-Hepa.

Validation of FastLec-Hepa. For a validation study, we obtained serum from CH patients at two locations: Nagoya City University Hospital and Hokkaido University Hospital (**Supplementary Fig. 10**). Staging of these patients ($n = 209$) by histological activity index (HAI) was conducted independently by two senior pathologists on ultrasonography-guided liver biopsy samples. F0–F1 was assigned in 82 cases (39.2%), F2 in 52 (24.9%), F3 in 40 (19.1%), and F4 (cirrhosis) in 35 (16.7%). Serum from healthy volunteers (with no history of any hepatitis virus infections) was obtained for analysis from two sites ($n = 48$ from National Institute of Advanced Industrial Science and Technology [AIST]: HV1; $n = 70$ from Nagoya City University: HV2). Their FastLec-Hepa counts

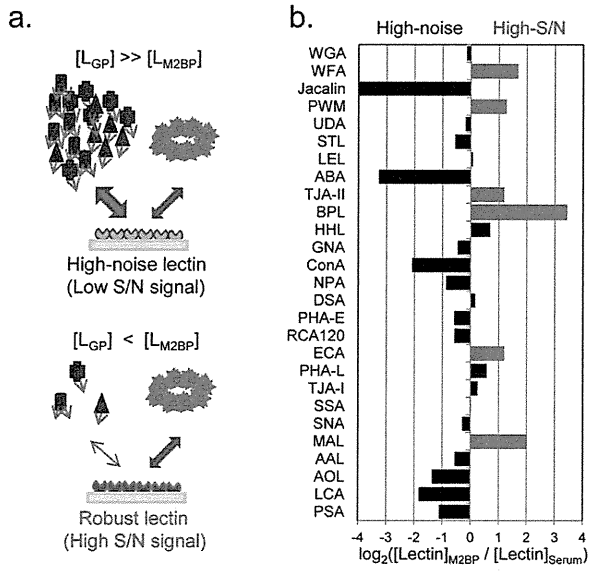

c.

	MAL	ECA	BPL	TJAII	PWM	WFA
1) Cirrhosis						
AUC	0.69	0.89	0.9	0.88	0.85	0.9
Sensitivity (%)	90	72	79	93	79	93
Specificity (%)	49	88	85	71	83	76
P-value	2.2×10^{-3}	3.2×10^{-10}	6.2×10^{-11}	5.1×10^{-10}	7.5×10^{-9}	5.5×10^{-11}
2) Severe fibrosis						
AUC	0.72	0.8	0.82	0.81	0.78	0.85
Sensitivity (%)	68	83	80	77	75	70
Specificity (%)	74	77	75	82	77	85
P-value	2.8×10^{-5}	6.2×10^{-9}	1.0×10^{-9}	2.0×10^{-9}	8.8×10^{-8}	3.0×10^{-11}
3) Significant fibrosis						
AUC	0.64	0.69	0.75	0.74	0.67	0.78
Sensitivity (%)	82	66	64	57	60	89
Specificity (%)	48	76	85	88	82	61
P-value	1.7×10^{-2}	1.3×10^{-3}	1.7×10^{-5}	4.6×10^{-5}	3.3×10^{-3}	1.3×10^{-6}

Figure 2 | Selection of the optimal lectin for the lectin-antibody sandwich immunoassay. (a) The kinetics of lectins binding to serum glycoproteins. The M2BP-binding lectins are divided into two categories: high-noise lectins and high signal-to-noise (S/N) lectins. The high-noise lectins bind to both M2BPs and abundant serum glycoproteins, causing a strong suppression of the M2BP–lectin interaction (see *top panel*). On the other hand, the number of binding targets in serum for the high S/N lectins is negligible, resulting in the specific interaction with the target M2BP (see *lower panel*). (b) Classification of M2BP-binding lectins. The high S/N lectins are those detecting M2BPs with at least twice the signal intensity seen for other serum glycoproteins. The classification strategy is summarized in **Supplementary Fig. 4**. (c) Diagnostic performance of 6 candidate lectins. *P*-values were determined using the nonparametric Mann–Whitney *U* test (Excel 2007, Microsoft).

(**Supplementary Table 1**) are also plotted in a box-whisker diagram in **Supplementary Fig. 11** along with that from a separate group of 1,000 healthy volunteers (HV3). Based on the calibration curve ([FastLec-Hepa counts]/10^6 = 1.027 × [rhM2BP] + 0.006 in **Fig. 3a, b**), the 75th percentiles of HVs of 64,205–107,617 and the 25th percentile of LC of 1,327,596 patients (see also **Supplementary Fig. 11**), we estimate the concentration of WFA$^+$-M2BP to be approximately 0.09 μg/ml in the serum of HV patients and > 1.0 μg/ml in that of LC patients. This means that the linear range shown in **Fig. 3a** is sufficient for accurate quantitation of WFA$^+$-M2BP in all serum samples. The analyses showed a gradual increase with the progression of liver fibrosis, but it did not correlate with the grade of hepatic activity defined by HAI scoring (**Supplementary Fig. 12**).

Next, we made a statistical comparison of FastLec-Hepa with other simple tests for liver fibrosis: the direct fibrosis marker hyaluronic acid (HA), the indirect fibrosis index FIB-4[26] and the glycan-based fibrosis index LecT-Hepa[18,27]. We enrolled 160 patients (F0−F1 = 66, F2 = 41, F3 = 33 and F4 = 20) whose age, platelet count, AST, ALT and HA levels were readily available (**Supplementary Fig. 10** and **Supplementary Tables 1 and 2**). As shown in **Fig. 4a**, the results of all the tests correlated well with the stage of fibrosis ($P < 0.0001$). However, an ROC analysis concluded that FastLec-Hepa detected cirrhosis with the highest diagnostic accuracy (**Fig. 4b** and **Table 1**). Notably, FastLec-Hepa distinguished between F3 and F4 with 90% sensitivity, 85% specificity, and with an AUC of 0.91. These results were superior to LecT-Hepa (sensitivity:

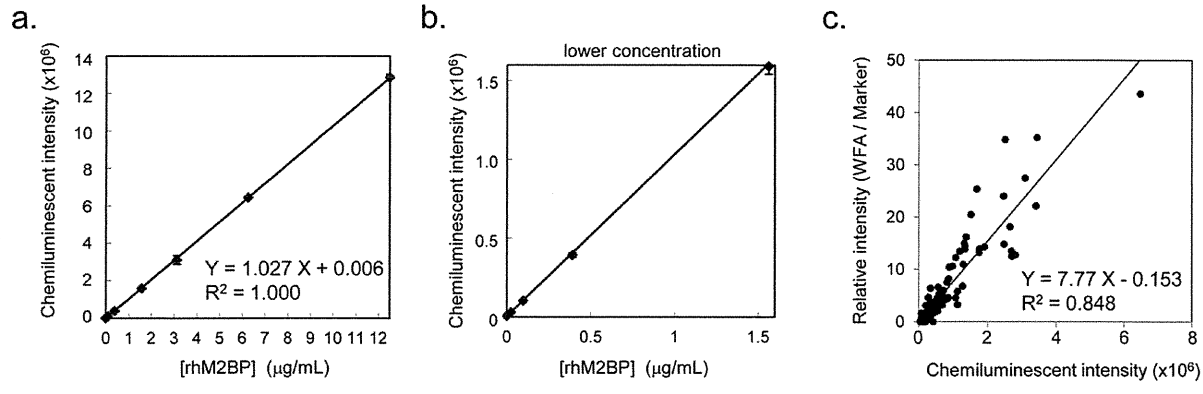

Figure 3 | Description of FastLec-Hepa, a fully automated WFA and anti-M2BP antibody sandwich immunoassay. (a) Standard curve for quantitation of WFA-binding rhM2BP. Plots for the lower concentration of rhM2BP are alternatively highlighted in (b). (c) Scatterplot comparison of WFA$^+$-M2BP data obtained from 125 different serum samples by both HISCL and a manual lectin microarray assay. The best-fit linear comparison with its correlation coefficient was calculated in Excel 2007 (Microsoft).

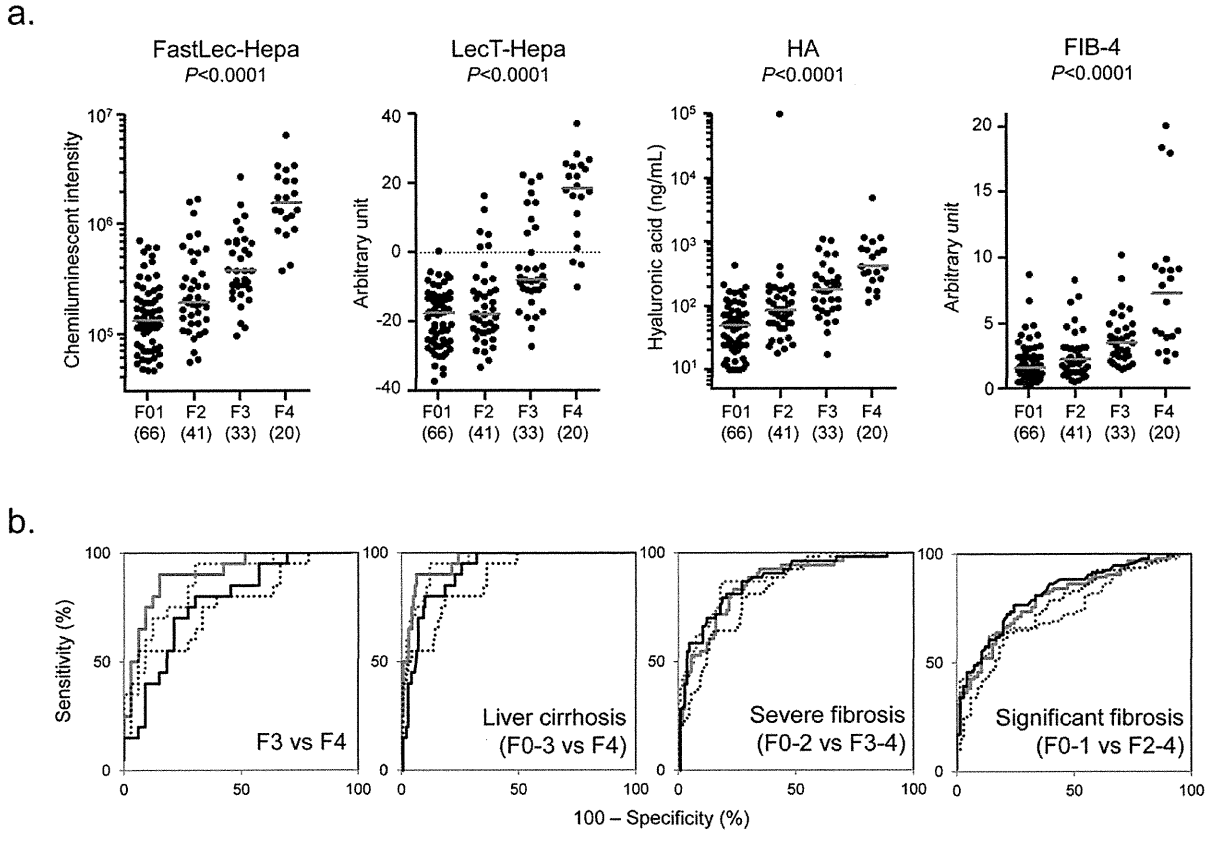

Figure 4 | Comparison of diagnostic performance of FastLec-Hepa, LecT-Hepa, HA, and FIB-4. (a) Scatterplots of the data obtained with FastLec-Hepa, LecT-Hepa, HA, and FIB-4 against the fibrosis score. Red horizontal lines represent the median. Correlation of the data with the progression of fibrosis was evaluated as significant differences in the medians relative to the fibrosis scores ($P < 0.0001$) by a nonparametric method, the Kruskal–Wallis one-way ANOVA. (b) Area under the receiver-operating characteristic (AUC-ROCs) curves of FastLec-Hepa, LecT-Hepa, HA, and FIB-4 for liver cirrhosis (F3 vs F4 or F0–3 vs F4), severe fibrosis (F0–2 vs F3–4), and significant fibrosis (F0–1 vs F2–4). FastLec-Hepa, LecT-Hepa, HA, and FIB-4 are indicated by a red solid line, red dotted line, black solid line, and black dotted line, respectively.

95%, specificity: 70%, and AUC: 0.87), FIB-4 (sensitivity: 55%, specificity: 94%, and AUC: 0.76), and HA (sensitivity: 80%, specificity: 70%, and AUC: 0.78).

Clinical utility of FastLec-Hepa: quantitative monitoring of antiviral therapy. To assess clinical utility, we examined two types of trials—short-interval evaluation and long-term follow-up—both of which are essential for following the patients receiving PEG-interferon-α and ribavirin therapy. For the first trial, we enrolled 41 patients with CHC who had previously undergone 48 weeks of therapy at Hokkaido University Hospital. According to the definition described in the **Methods**, 26 and 15 of them were judged as SVR and NVR/relapse (non-SVR), respectively. For each patient, we performed FastLec-Hepa on serum samples, which were collected just before treatment (Pre) and within a short period (12–22 weeks) after treatment (Post) (**Fig. 5a**). We found a marked decrease from Pre to Post counts ($P = 0.0061$) in SVR patients, but no apparent change for non-SVR patients ($P = 0.9780$) (**Fig. 5b**). Specifically, a median percent decrease of 31% was found for SVR patients (median Pre-count of 161,053 and median Post-count of 110,739), while the level for non-SVR patients was essentially constant. These results show that the assay can evaluate the effect of therapy within a short period after treatment. This is an important advance, because the ALT levels of non-SVR, as well as SVR, are mostly decreased into the range of 10–64 IU/ml during this period (**Fig. 5c**)[5]. In fact, changes in the FastLec-Hepa counts did not correlate with those in the ALT counts (**Supplementary Fig. 13**), thereby invalidating ALT-dependent fibrosis assays, including FIB-4 (**Fig. 5d**).

In support of our finding that the FastLec-Hepa counts correlate excellently with the stage of fibrosis, we found a strong correlation between the histopathological scores and the median of the $\log_{10}$[FastLec-Hepa] counts (**Fig. 5e**). These correlations were approximated to two linear equations: $y = 0.23x + 4.9$ for F0 to F3, and $y = 0.58x + 3.8$ for F3 to F4 histology. This means that FastLec-Hepa can reliably reproduce the assessment of therapeutic effects, which were previously drawn from histopathological scoring[9]. Indeed, the median changes in fibrosis obtained by FastLec-Hepa analysis were about −0.295 stages/year for SVR and 0.010 stages/year for non-SVR (**Fig. 5f**). These data were consistent with the rate of fibrosis progression and regression determined by Shiratori *et al*[9].

For the second trial, we enrolled 6 HCV patients (SVR = 3 and non-SVR = 3) with advanced fibrosis who completed 48 weeks of therapy at Nagoya City University Hospital. Sera were collected before therapy and at 0, 1, 3, and 5 years after the end of therapy (see **Fig. 5g**). FastLec-Hepa counts in SVR patients gradually decreased and reached below the median of F0 patients within 3 years. However, those in non-SVR patients remained above the median for F3 patients during the follow-up period (**Fig. 5h**).

Table 1 | Diagnostic performance of fibrosis markers

n = 160	FIB-4	HA	LecT-Hepa	FastLec-Hepa
a) Significant fibrosis (F0–1 vs F2–4)				
AUC	0.76	0.82	0.76	0.79
(95% CI)	(0.68–0.83)	(0.76–0.89)	(0.69–0.83)	(0.72–0.86)
Diagnostic sensitivity (%)	64	77	63	81
Diagnostic specificity (%)	79	76	86	67
Youden's index (%)	43	52	49	48
b) Severe fibrosis (F0–2 vs F3–4)				
AUC	0.83	0.87	0.88	0.84
(95% CI)	(0.76–0.89)	(0.81–0.93)	(0.82–0.93)	(0.77–0.91)
Diagnostic sensitivity (%)	81	81	87	83
Diagnostic specificity (%)	71	79	81	77
Youden's index (%)	52	61	68	60
c) Liver cirrhosis (F0–3 vs F4)				
AUC	0.88	0.91	0.95	0.96
(95% CI)	(0.80–0.95)	(0.86–0.96)	(0.92–0.99)	(0.93–0.99)
Diagnostic sensitivity (%)	80	80	95	90
Diagnostic specificity (%)	81	90	88	94
Youden's index (%)	61	70	83	84
d) Liver cirrhosis (F3 vs F4)				
AUC	0.76	0.78	0.87	0.91
(95% CI)	(0.63–0.90)	(0.65–0.90)	(0.77–0.97)	(0.82–0.99)
Diagnostic sensitivity (%)	55	80	95	90
Diagnostic specificity (%)	94	70	70	85
Youden's index (%)	49	50	65	75

Interestingly, HCC had developed in two non-SVR patients whose FastLec-Hepa counts remained above the median of F4 patients throughout. Other fibrosis indices, such as FIB-4 and biochemical parameters (ALT and AST), did not distinguish between SVR and non-SVR or appear to predict this occurrence (**Fig. 5i-k**).

Discussion

We have described the development and use of a fully automated, glycan-based immunoassay termed FastLec-Hepa, for the evaluation of liver fibrosis. A high degree of reliability in the quantitative aspects of this method should establish it as a clinically significant test,

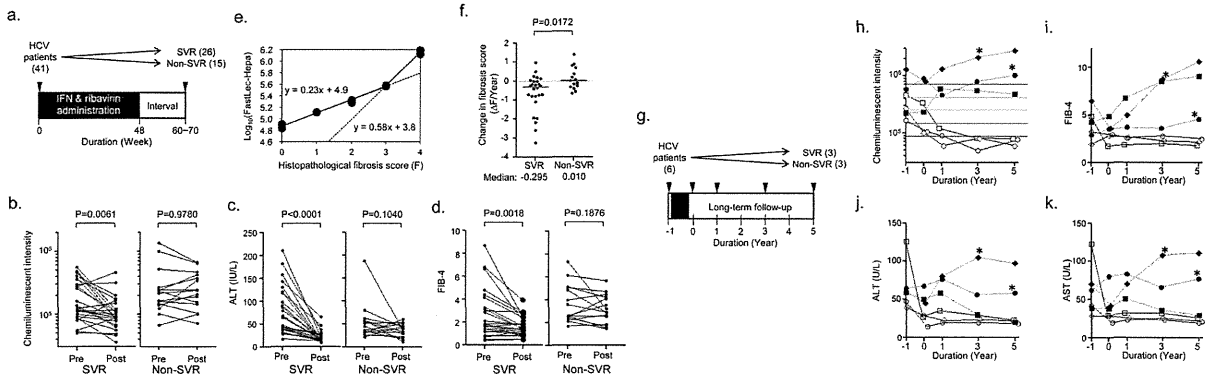

Figure 5 | Evaluation of the curative effect of interferon therapy by FastLec-Hepa. (a) Validation of FastLec-Hepa in short-interval evaluation. The numbers in parentheses represent the number of patients participated in this experiment. Arrowheads indicate the timing of blood collection. At week 0, blood was collected immediately before the treatment. Black box indicates the period of PEG-interferon-α and ribavirin therapy. Changes in the FastLec-Hepa counts (b), ALT (c), and the FIB-4 index (d) in patients with sustained virologic response (SVR) and relapse/nonresponders (non-SVR) during interferon therapy. The *P*-value was determined by a nonparametric method, the Wilcoxon matched pairs signed-rank test. (e) Dot-plot representation of the histopathological fibrosis score and the medians of FastLec-Hepa counts. Best-fit linear curves were calculated in Excel 2007 (Microsoft) allowing conversion of the FastLec-Hepa counts into fibrosis score. (f) Yearly changes in the converted fibrosis score. Changes for patients with SVR and non-SVR are indicated in the dot plots. Red horizontal lines represent the median. The *P*-value was determined by the Mann–Whitney *U* test. (g) Validation of FastLec-Hepa in long-term follow-up. The numbers in parentheses represent the number of patients participated in this experiment. Arrowheads indicate the timing of blood collection. At year -1 and 0, the blood was collected immediately before and after the treatment, respectively. Black box indicates the period of PEG-interferon-α and ribavirin therapy. Yearly changes of FastLec-Hepa counts (h), FIB-4 index (i), ALT (j), and AST (k) in individual patients after therapy. The five colored lines in (h) represent the median values obtained for each fibrosis stage (red, F4; orange, F3; green, F2; cyan, F1; blue, F0). Closed and opened symbols indicate the data obtained from non-SVR and SVR patients, respectively. * indicates the period when the development of HCC was found.

particularly for revealing and managing patients at a high risk of progression to liver complications such as HCC and related life-threatening events. The most striking advantage of FastLec-Hepa is not only its simplicity but also its capacity to provide fibrosis read-outs that are not influenced by fluctuations in the ALT value or inflammation, both of which can cause falsely high estimates in most of the other fibrosis tests available[10]. In fact, our study has illustrated robust capacity of FastLec-Hepa to evaluate the effects of antiviral therapy and subsequent disease progression in both the short and long term.

Many retrospective and prospective studies have demonstrated that achieving SVR through the PEG-interferon-α/ribavirin treatment significantly reduces liver-related morbidity and mortality (i.e., hepatic decompensation, HCC, and liver-related death)[28–30]. As this combination therapy is effective in only about 50% of patients with HCV genotype 1, new agents[1] and targets[31] for antiviral treatments of HCV have been developed to achieve SVR more effectively after the therapy. Long-term follow-ups often show that the risk of disease progression is significantly high in patients with non-SVR after PEG-interferon-α/ribavirin treatment. Furthermore, the development of HCC in patients with SVR remains at a significant cumulative rate (2%)[28,30,32,33]. For these reasons, a new data-mining model using individual factors (age, platelet count, serum albumin and AST) was developed recently to identify patients at a high risk of HCC development[34]. This is, however, a statistical procedure for estimating the chance of disease progression, and there is not a direct evaluation of fibrosis. In the present report, we performed a long-term retrospective study with serially collected sera from SVR and non-SVR patients, in which we showed the potential use of FastLec-Hepa for improved prognostic accuracy. Indeed, recent advances in the development of antifibrotic agents lead us to expect the therapeutic elimination of health risks associated with HCC and decompensation[35]. Moreover, we expect that FastLec-Hepa will be proved for its usefulness in rapid evaluation of progression and regression of fibrosis in clinical trials of newly developed antifibrotic agents. Hence, FastLec-Hepa should be very useful for fibrosis stage screening and evaluation of disease progression in untreated individuals or patients under or after treatment, as well as evaluation of the most recently developed drugs.

It is important to note that FastLec-Hepa has many merits, including speed (possibly 1,000 assays per day) and full automation for measurement of a serological glycobiomarker: these attributes will enable retrospective studies with valuable serum specimens that have been collected previously. In addition, our recently developed calibrator for FastLec-Hepa will improve traceability and enable simultaneous assay and data storage in multiple diagnostic facilities. The data obtained with diluted serum samples demonstrated a high level of assay reproducibility and a very favorable linear detection range (**Supplementary Fig. 14**). Furthermore, we found an excellent agreement between assay values for serum and plasma prepared simultaneously from the same patient. Presently, we have about 10,000 sera and plasma available with detailed clinical notes collected in more than 10 facilities in Japan, and a series of retrospective studies is under way. We will shortly conclude licensing of our system for clinical implementation, based largely on the trials of the present study. In contrast to this, the majority of recent noninvasive techniques are currently shifting to physical measurements such as FibroScan, acoustic radiation force impulse[36] and real-time strain elastography[37]. Any on-site assay of large numbers of blood samples should provide a diagnostic value comparable to that of FibroTest, and a direct comparison in the same patient group will be necessary to evaluate this. We note here that according to a recent statistical validation method[38], predicted AUC of the diagnostic value of FibroTest for detection of advanced fibrosis in our sample set (DANA score = 1.81) was approximately 0.77, which was comparable to the AUC of FastLec-Hepa we obtained (0.79).

FastLec-Hepa has adopted a new paradigm for clinical diagnosis, "glyco-diagnosis", which is based on the quantity and quality of protein glycosylation patterns that well indicate disease progression. To detect such changes in glycosylation by conventional methods (e.g., mass spectrometry, liquid chromatography, or capillary electrophoresis), it is absolutely necessary to liberate the glycans of interest from their protein linkages[15,17,39]. It is possible to employ an alternative technology, which is based on a lectin–antibody sandwich immunodetection system for intact glycoproteins bearing disease-specific glyco-alterations. Such assays have been used to detect changes in fucosylation of *N*-linked glycans, which are associated with liver disease. However, in the present study, fucose-binding lectins were classified as "high noise" (**Fig. 2b**), and thus an enrichment of the target protein was the essential process in the assay. Lectin-overlay detection is performed typically after on-plate enrichment of the target glycoproteins by an immobilized antibody. In such cases, detection relies on a low avidity (high dissociation rate) between the captured glycoprotein and the overlaid lectin probe (see *right* of **Supplementary Fig. 3b**). These kinetic considerations essentially eliminate the use of an automated bedside clinical chemistry analyzer. Even though a fucose-binding lectin was immobilized on the beads (see *left* of **Supplementary Fig. 3b**), it still remains a problem for reliable quantitation by autoanalyzer. Our previous system LecT-Hepa[16,18,19,26], which detects the level of fucosylated α1-acid glycoprotein, requires enrichment of the protein prior to the assay.

In the present study, we have developed a strategy to overcome these problems in glyco-diagnosis associated with clinical implementation, and realized a rapid "on-site diagnosis" system (17 min, within the minimum time required for single assay by HISCL), based on analysis of a glycomarker (**Supplementary Fig. 1**). The strategy for selecting the most robust lectin led us to WFA, and away from the use of fucose-binding lectins, for the direct measurement system (**Fig. 2**). The diagnostic utility of M2BP, a protein resembling "sweet-doughnut"[20], brought a favorable density and orientation of the disease-related glycan on the homomultimer. These characteristic structures resulted in a major increase in the avidity of M2BP for the plated WFA. The resulting glycan–lectin interaction, which is remarkably strong and specific, made it possible to develop the rapid and highly sensitive assay (see *left* of **Supplementary Fig. 3b**). We believe that this unique strategy will revolutionize the use of glyco-diagnosis in clinical medicine and potentially provide a framework for the development of a new generation of biomarker assays.

Methods

Patient samples, biochemical parameters and indices. Patients with chronic hepatitis were enrolled at Nagoya City University Hospital and Hokkaido University Hospital. Healthy volunteers as the controls were randomly selected in Nagoya City University Hospital (70 individuals) and AIST (48 individuals). The institutional ethics committees at Nagoya City University Hospital, Hokkaido University Hospital, and AIST approved this study, and informed consent for the use of their clinical specimens was obtained from all participants before the collection. In addition, we used 1,000 serum samples from virus-negative Caucasians as the normal population, which were purchased from Complex Antibodies Inc. (Fort Lauderdale, FL) and collected under IRB-approved collection protocols. Fibrosis was graded in the patients according to the histological activity index (HAI) using biopsy or surgical specimens. Biopsy specimens were classified as follows: F0, no fibrosis; F1, portal fibrosis without septa; F2, few septa; F3, numerous septa without cirrhosis; and F4, cirrhosis. The three diagnostic targets in this study were defined as significant fibrosis: F2+F3+F4; severe fibrosis: F3+F4; and cirrhosis: F4. Hepatic inflammation was also assessed according to the HAI, as follows: A0, no activity; A1, mild activity; A2, moderate activity; and A3, severe activity. Cirrhosis was confirmed by ultrasonography (coarse liver architecture, nodular liver surface, and blunt liver edges), evidence of hypersplenism (splenomegaly on ultrasonography) and/or a platelet count of $< 100{,}000/mm^3$. Virological responses during PEG-interferon-α and ribavirin therapy were defined as follows[5]: SVR, absence of HCV RNA from serum 24 weeks following discontinuation of therapy; nonresponder, failure to clear HCV RNA from serum after 24 weeks of therapy; relapse, reappearance of HCV RNA in serum after therapy was discontinued. For all patients, age and sex were recorded and serum levels of the following were analyzed: aspartate aminotransferase (AST), alanine aminotransferase (ALT), γ-glutamyltransferase (GGT), total bilirubin,

albumin, cholinesterase, total cholesterol, platelet count (PLT), hyaluronic acid (HA). The FIB-4 index was calculated as follows: [age (years) × AST (U/L)]/[platelets (10^9/L) × ALT (U/L)$^{1/2}$][26]. Fibrosis-specific glyco-alteration of α1-acid glycoprotein was determined by lectin–antibody sandwich immunoassays with a combination of three lectins (*Datura stramonium* agglutinin (DSA), *Maackia amurensis* leukoagglutinin (MAL), and *Aspergillus oryzae* lectin (AOL))[16]. All assays used an automated chemiluminescence enzyme immunoassay system (HISCL-2000i; Sysmex Co., Kobe, Japan)[18].

Enrichment of M2BP from serum. An automated protein purification system (ED-01; GP BioSciences Ltd., Yokohama, Japan) was used to immunoprecipitate M2BP from serum specimens. In brief, sera (2 μl) were diluted 10-fold with PBS/0.2%(w/v) SDS, heated at 95°C for 20 min, mixed with 10 μl of Triton X-100 in TBS (TBSTx) and injected into a 96-well SUMILON microtiter plate (Sumitomo Bakelite Co., Ltd., Tokyo, Japan). The plate and working reagents, including biotinylated anti-M2BP antibody (10 ng/μl), streptavidin-coated magnetic beads, washing buffer (1% TBSTx) and elution buffer (TBS containing 0.2% SDS), were loaded into the system. This generated 110 μl of purified M2BPs per serum sample (96 samples in 3.5 h).

Western blot analysis. Anti-human M2BP polyclonal antibody was purchased from R&D Systems, Inc. (Minneapolis, MN) and biotinylated with Biotin Labeling Kit – NH_2 (Dojindo Laboratories, Kumamoto, Japan). Purified serum M2BPs were electrophoresed under reducing conditions on 5–20% polyacrylamide gels (DRC, Tokyo, Japan) and transferred to PVDF membranes. After treatment with Block Ace® (DS Pharma Biomedical Co., Ltd., Osaka, Japan), the membranes were incubated with biotinylated anti-M2BP polyclonal antibody, and then with alkaline phosphatase-conjugated streptavidin (1/5000 diluted with TBST; ProZyme, Inc., San Leandro, CA). The membranes were incubated with Western Blue stabilized substrate for alkaline phosphatase (Promega, Madison, WI).

Lectin microarray analysis. Enriched M2BPs were analyzed with an antibody-overlay lectin microarray[24]. Purified protein (14 μl) was diluted to 60 μl with PBS containing 1%(v/v) Triton X-100 (PBSTx); this was applied to a LecChip™ (GP BioSciences Ltd.), which included three spots of 45 lectins in each of seven reaction wells. After incubation for 12 h at 20°C, 2 μl of human serum IgG (10 mg/ml) was added to the reaction solution on each chip and incubated for 30 min. The reaction solution was then discarded, and the chip was washed three times with PBSTx. Subsequently, 60 μl (200 ng) of biotinylated anti-human M2BP in PBSTx was applied to the chip, and incubated for 1 h. After three washes with PBSTx, 60 μl (400 ng) of a Cy3-labeled streptavidin (GE Healthcare, Buckinghamshire, UK) solution in PBSTx was added and incubated for 30 min. The chip was rinsed with PBSTx, scanned with an evanescent-field fluorescence scanner (GlycoStation™ Reader1200; GP BioSciences Ltd.) and analyzed with the Array Pro Analyzer software package, version 4.5 (Media Cybernetics, Inc., Bethesda, MD). The chip was scanned with the gain set to register a maximum net intensity < 40,000 for the most intense spots. The net intensity value for each spot was calculated by subtracting the background value from the signal intensity value. The relative intensity of lectin-positive samples was determined from the ratio of their fluorescence to the fluorescence of the internal-standard lectin, DSA.

Quantitation of *Wisteria floribunda* agglutinin (WFA)-binding M2BP. Serum was pretreated as described above under enrichment of M2BP from serum. Pretreated samples (50 μl) were diluted with an equal volume of starting buffer (0.1%(w/v) SDS in PBSTx), added to the WFA-coated agarose in a microtube (20 μl slurry; Vector Lab., Burlingame, UK), and incubated at 4°C for 5 h with gentle shaking. After centrifugation of the reaction solution at 2000 × *g* for 10 min, the supernatant was removed to a new microtube. The precipitate was suspended in 50 μl of the starting buffer, recentrifuged and this second supernatant combined with the first (designated as path-through fraction T). The precipitate was then washed with 200 μl of the starting buffer and the bound glycoproteins were eluted with 60 μl of 200 mM galactosamine/0.02%(w/v) SDS in PBS (designated as elution fraction E). M2BP was immunoprecipitated from fractions T and E and examined by electrophoresis under reducing conditions on 5–20% gradient SDS–polyacrylamide gels.

WFA-antibody sandwich ELISA. Flat-bottomed 96-well streptavidin-precoated microtiter plates (Nunc, Int., Tokyo, Japan) were treated with biotinylated WFA (Vector, 250 ng/well) for 1 h at room temperature. The plates were incubated with the diluted serum samples (50 μl) in PBS containing 0.1%(v/v) Tween20 (PBS-t) for 2 h at room temperature and then with 50 ng/well of the anti-human M2BP polyclonal antibody, in PBS-t for 2 h at room temperature. The plates were washed extensively and then incubated with 50 μl of horseradish peroxidase (HRP)-conjugated anti-mouse IgG (Jackson ImmunoResearch Laboratories Inc., Philadelphia, PA) at 1:10,000 in PBS-t for 1 h at room temperature. The substrate 3,3′,5,5′-tetramethylbenzidine (Thermo Fisher Scientific, Fremont, CA) solution (100 μl) was added to each well. The enzyme reaction was stopped by adding 100 μl of 1 M sulfuric acid, and the optical density measured at 450 nm.

WFA-antibody sandwich immunoassay by HISCL. The fibrosis-specific form of glycosylated M2BP was measured based on a sandwich immunoassay approach. Glycosylated M2BP was captured by WFA immobilized on magnetic beads, and the bound product was assayed with an anti-human M2BP monoclonal antibody linked to alkaline phosphatase (ALP-αM2BP). Two reagent packs (M2BP-WFA detection pack and a chemiluminescence substrate pack) were loaded in the HISCL. The detection pack comprised three reagents: a reaction buffer solution (R1), a WFA-coated magnetic beads solution (R2) and an ALP-αM2BP solution (R3). The chemiluminescence substrate reagent pack contained a CDP-Star substrate solution (R4) and a stopping solution (R5). Typically, serum (10 μl) was diluted to 60 μl with R1 and then mixed with R2 (30 μl). After the binding reaction, R3 (100 μl) was added to the reaction solution. The resultant conjugates were magnetically separated from unbound components, and mixed well with R4 (50 μl) and R5 (100 μl) before reading of the fluorescence. The chemiluminescent intensity was acquired within a period of 17 min in the operation described above. The reaction chamber was kept at 42°C throughout.

Statistics. Statistical analyses and graph preparation used Dr. SPSS II Windows software (SPSS Co., Tokyo, Japan), GraphPad Prism 5.0 (GraphPad Software Inc., La Jolla, CA), and Windows Excel 2007. This facilitated selection of the optimal lectin for analysis of fibrosis and a comparison of the diagnostic value of other serological fibrosis markers and indices. Because the data distribution for each parameter was non-Gaussian, the *P*-values were determined by nonparametric tests, such as the Mann–Whitney *U* test and Wilcoxon signed-rank test. Correlations with liver fibrosis were estimated as the significance of differences among the staging groups (F0–1, F2, F3, and F4) determined by Kruskal–Wallis nonparametric one-way analysis of variance. To assess classification efficiencies for detecting significant fibrosis, severe fibrosis and cirrhosis, the receiver-operating characteristic (ROC) curve analysis was also carried out to determine the area under the curve (AUC) values. Cutoff values obtained from Youden's index were used to classify patients. Diagnostic accuracy was expressed in terms of specificity, sensitivity and AUC.

1. "Nature Outlook Hepatitis C" edited by Brody, H. *et al. Nature* **474**, S1–S21 (2011).
2. Ge, D. *et al.* Genetic variation in IL28B predicts hepatitis C treatment-induced viral clearance. *Nature* **461**, 399–401 (2009).
3. Suppiah, V. *et al.* IL28B is associated with response to chronic hepatitis C interferon-alpha and ribavirin therapy. *Nat. Genet.* **41**, 1100–1104 (2009).
4. Tanaka, Y. *et al.* Genome-wide association of IL28B with response to pegylated interferon-alpha and ribavirin therapy for chronic hepatitis C. *Nat. Genet.* **41**, 1105–1109 (2009).
5. Ghany, M. G., Strader, D. B., Thomas, D. L. & Seeff, L. B. Diagnosis, management, and treatment of hepatitis C: an update. *Hepatology* **49**, 1335–1374 (2009).
6. Afdhal, N. H. *et al.* hepatitis C pharmacogenetics: state of the art in 2010. *Hepatology* **53**, 336–345 (2011).
7. Peng, C. Y., Chien R. N. & Liaw, Y. N. Hepatitis B virus-related decompensated liver cirrhosis: benefits of antiviral therapy. *J. Hepatol.* **57**, 442–450 (2012).
8. Chang, T. T. *et al.* Long-term entecavir therapy results in the reversal of fibrosis/cirrhosis and continued histological improvement in patients with chronic hepatitis B. *Hepatology* **52**, 886–893 (2010).
9. Shiratori, Y. *et al.* Histologic improvement of fibrosis in patients with hepatitis C who have sustained response to interferon therapy. *Ann. Intern. Med.* **132**, 517–524 (2000).
10. Castera, L. Non-invasive assessment of liver fibrosis in chronic hepatitis C. *Hepatol. Int.* **5**, 625–634 (2011).
11. Imbert-Bismut, F. *et al.* Biochemical markers of liver fibrosis in patients with hepatitis C virus infection: a prospective study. *Lancet* **357**, 1069–1075 (2001).
12. Calès, P. *et al.* A novel panel of blood markers to assess the degree of liver fibrosis. *Hepatology* **42**, 1373–1381 (2005).
13. Castera, L. *et al.* Prospective comparison of two algorithms combining non-invasive methods for staging liver fibrosis. *J. Hepatol.* **52**, 191–198 (2010).
14. Boursier, J. *et al.* Comparison of eight diagnostic algorithm for liver fibrosis in hepatitis C: new algorithms are more precise and entirely noninvasive. *Hepatology* **55**, 58–67 (2012).
15. Callewaert, N. *et al.* Noninvasive diagnosis of liver cirrhosis using DNA sequencer-based total serum protein glycomics. *Nat. Med.* **10**, 429–434 (2004).
16. Kuno, A. *et al.* Multilectin assay for detecting fibrosis-specific glyco-alteration by means of lectin microarray. *Clin. Chem.* **57**, 48–56 (2011).
17. Vanderschaeghe, D. *et al.* High-throughput profiling of the serum N-glycome on capillary electrophoresis microfluidics systems: toward clinical implementation of GlycoHepatoTest. *Anal. Chem.* **82**, 7408–7415 (2010).
18. Kuno, A. *et al.* LecT-Hepa: A triplex lectin-antibody sandwich immunoassay for estimating the progression dynamics of liver fibrosis assisted by a bedside clinical chemistry analyzer and an automated pretreatment machine. *Clin. Chim. Acta* **412**, 1767–1772 (2011).
19. Du, D. *et al.* Comparison of LecT-Hepa and FibroScan for assessment of liver fibrosis in hepatitis B virus infected patients with different ALT levels. *Clin. Chim. Acta* **413**, 1796–1799 (2012).
20. Sasaki, T., Brakebusch, C., Engel, J. & Timpl, R. Mac-2 binding protein is a cell-adhesive protein of the extracellular matrix which self-assembles into ring-like structures and binds beta1 integrins, collagens and fibronectin. *EMBO J.* **17**, 1606–1613 (1998).
21. Iacovazzi, P. A. *et al.* Serum 90K/MAC-2BP glycoprotein in patients with liver cirrhosis and hepatocellular carcinoma: a comparison with alpha-fetoprotein. *Clin. Chem. Lab. Med.* **39**, 961–965 (2001).